International Journal of Nanomedicine Dovepress

Open Access Full Text Article ORIGINAL RESEARCH

Resveratrol-Loaded Versatile Nanovesicle for Alopecia Therapy via Comprehensive Strategies

Xuefei Zhang[1,2], Jiabao Hao[1], Tianli Lu[1], Yating Dong[1], Yingying Sun[1], Yingjun Yu[1], Shuxuan Li[1], Shihui Yu[1,3,4], Haiyan Hu[1,3,4]

[1]School of Pharmaceutical Sciences, Sun Yat-Sen University, Guangzhou, Guangdong Province, People's Republic of China; [2]School of Traditional Dai-Thai Medicine, West Yunnan University of Applied Sciences, Jinghong, Yunnan Province, People's Republic of China; [3]State Key Laboratory of Anti-Infective Drug Discovery and Development, School of Pharmaceutical Sciences, Sun Yat-sen University, Guangzhou, Guangdong Province, People's Republic of China; [4]Guangdong Provincial Key Laboratory of Chiral Molecules and Drug Discovery, Sun Yat-Sen University, Guangzhou, Guangdong Province, People's Republic of China

Correspondence: Haiyan Hu, Email lsshhy@mail.sysu.edu.cn

Introduction: Alopecia is a systemic disease with multiple contributing factors. Effective treatment is challenging when only hair growth mechanisms are targeted while ignoring the role of maintaining hair follicle microenvironment homeostasis, which is crucial for cell growth and angiogenesis. Oxidative stress and inflammation are major disruptors of this microenvironment, leading to inhibited cell proliferation and compromised hair follicle circulation. Drugs with antioxidant and anti-inflammatory effects could potentially restore microenvironment homeostasis, offering a promising strategy for alopecia treatment.

Methods: Resveratrol (RES), a potent antioxidant and anti-inflammatory agent, was selected as the model drug and encapsulated into an active carrier—PPD-Lip to create PPD-Lip@RES. The efficacy of PPD-Lip@RES was comprehensively evaluated in both in vitro and in vivo aspects, and its underlying mechanism was also primarily explored.

Results: PPD-Lip@RES promoted the proliferation and migration of dermal papilla cells, up-regulated the expression of positive hair growth regulators, and facilitated angiogenesis. It also activated hair follicle stem cells by increasing the expression of Ki67, K5, β-catenin, CD31, and CK19. In the telogen effluvium model, PPD-Lip@RES resulted in more robust hair regeneration, with less hair shedding compared to the minoxidil group. Furthermore, it showed significant therapeutic effects in severe androgenetic alopecia, outperforming finasteride and even the healthy control group.

Conclusion: The results suggested that PPD-Lip@RES, as a systemic intervention strategy, could effectively facilitate hair growth by targeting both the pathological and physiological processes involved in hair loss. Its superior performance in both telogen effluvium and androgenetic alopecia models indicates its potential as an advanced treatment option for alopecia.

Keywords: hair loss, microenvironment, antioxidant, anti-inflammatory, nanocarrier

Introduction

Alopecia, an increasingly prevalent health issue among contemporary young and middle-aged people, leads to significant negative psychological effects, such as anxiety, inferiority, self-doubt, and even depression.[1] With the intensification of mental stress and environmental pollution, the incidence rate of alopecia is rapidly increasing and developing a trend toward younger ages, resulting in a rising demand for treatment. Hair loss as a progressive disease, unless early intervention, will become increasingly severe, eventually balding, and then aggravating the negative impact on the patient's physical and mental health. Currently, there are two mainstream drugs approved by the Food and Drug Administration (FDA) for the treatment of hair loss: topical minoxidil and oral finasteride. However, hair loss treatment would take a long time, long-term use of minoxidil and finasteride might have toxic side effects. In addition, compared to the complex etiology of hair loss, both two drugs have a single mechanism and hence establish the limited effectiveness in treating hair loss.[2] Therefore, it is urgent to develop a safe and effective alternative comprehensive therapy addressing multiple pathological factors for hair loss.

Received: 10 July 2024
Accepted: 20 November 2024
Published: 24 December 2024

Alopecia is a systemic disease caused by a variety of factors, mainly including inhibition of cell proliferation, insufficient vascularization, and hair follicle microenvironment disorders, etc. Most treatment strategies only focus on promoting cell proliferation and angiogenesis but neglect the effect of hair follicle microenvironment homeostasis on promoting cell proliferation and angiogenesis, ultimately reducing the effectiveness of hair loss treatment. That is, the homeostasis of the hair follicle microenvironment was essential to maintain the normal cycle of hair follicles. The disordered microenvironment around hair follicles would fail to activate hair follicle stem cells (HFSCs), suppress cell growth and angiogenesis, preventing the transition of hair follicles from the telogen phase to the anagen phase and ultimately inhibiting hair growth.

Excessive inflammation and oxidative stress are the key causes of abnormal hair follicle microenvironment, which cannot be ignored.

Typically, the excessive accumulation of reactive oxygen species (ROS) can be caused by multiple factors, such as the closed state of the hair follicle microenvironment. The high vascularization and an exceedingly high proliferation rate of matrix cells in hair follicles brings about the production of a substantial amount of ROS. Moreover, ultraviolet radiation and pollutants could also cause the generation of ROS.[3] The excessive accumulation of ROS damages the function of various cells in hair follicles, including increasing β-galactosidase activity, up-regulating aging-related proteins in dermal papilla cells (DPCs), accelerating DPCs aging, and then inducing the secretion of signaling molecules that inhibit hair follicle activation and hence hinder hair growth.[4,5] Besides, oxidative stress was responsible for the loss of blood vessels by damaging vascular endothelial cells and hence cutting off the supply of nutrients and growth factors provided by the blood vessels around the hair follicles.

Inflammation around hair follicles was another inducement of hair loss,[6] which could damage the microenvironment of HFSCs through interferon-induced cytokine expression, but also serve as a trigger for disrupting the homeostasis of hair follicle microenvironment, impact the normal function of hair follicles, promote the transition of hair follicles from the anagen to the catagen phase, thereby inhibiting hair growth, and ultimately lead to hair loss. In addition, the local chronic inflammation could also stimulate the production of ROS, leading to the vicious cycle of hair follicle microenvironment disorder.[3] Therefore, drugs with anti-inflammatory activity were expected to eliminate inflammatory factors, restore the homeostasis of hair follicles microenvironment, and promote hair growth.[7]

In summary, the causes of hair loss are complex, apart from promoting cell proliferation and angiogenesis, eliminating ROS and inflammatory factors in the hair follicle microenvironment is of great value in maintaining cell growth and various functions, and promoting hair growth. Therefore, a comprehensive strategy that could restore hair follicle homeostasis through antioxidation and anti-inflammation, promoting the proliferation and migration of DPCs and facilitating angiogenesis around the hair follicle and so on, is expected to demonstrate good hair loss treatment effects.

Resveratrol (RES), a naturally non-flavonoid polyphenol compound, has excellent anti-oxidant and anti-inflammatory activities. It has garnered considerable attention in cosmetic research and been widely used. Studies have found that RES could improve hair loss in patients with polycystic ovaries.[8] Zhang et al found that RES could promote the proliferation of DPCs,[9] prevent H_2O_2-induced oxidative damage to DPCs. Juchaux et al combined 5% 2,4-diethylpyridine dicarboxylate with 0.25% RES,[10] which significantly increased the hair density of women after 1.5 months treatment. Chisato et al found that RES could up-regulate the expression of β-catenin,[11] activate the Wnt/β-catenin signaling pathway, and drive hair follicles from the telogen phase to the anagen phase. These studies suggested that RES may be a potential candidate for treating alopecia.

Since alopecia occurs on the scalp, topical administration of RES appears promising for improving therapeutic effect and reducing systemic toxicity by increasing the drug content in the scalp.[12] However, the RES was highly lipophilic (log P = 3.32) and slightly soluble, which has poor skin permeability by direct use. Compared with the method of using organic solvent for drug delivery, loading RES into nanovesicles might significantly improve the solubility, stability, and skin penetration of RES,[13] hence raising its biological activity. Our previous study has found that by substituting cholesterol with protopanaxadiol (PPD) as the liposomal membrane material, PPD-Lip not only avoids the adverse effects associated with cholesterol but also effectively delivers drugs to the deep skin and maintains prolonged retention within hair follicles. Furthermore, PPD serves as both an active ingredient for treating hair loss, making PPD-Lip a promising system for the targeted delivery of compounds like RES. In addition, the natural origin of PPD contributes to

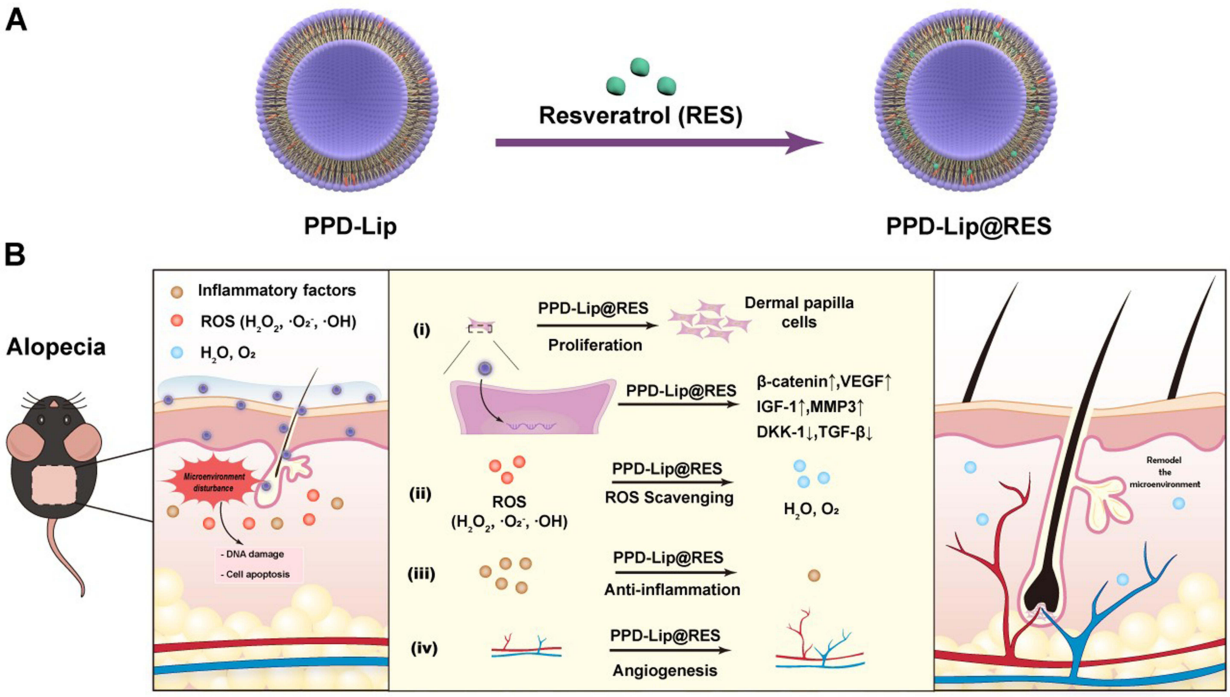

Scheme 1 Schematic of the construction of PPD-Lip@RES (**A**) and its mechanism (**B**) for alopecia treatment.

the more excellent biocompatibility and biodegradability of PPD-Lip than some synthetic materials, making it safer for prolonged use. This combination of targeted delivery, skin permeability, and high safety profile positions PPD-Lip as an effective and reliable delivery system for therapeutic compounds targeting the hair follicle and deep skin layers.

Based on the above assumptions, this project is intended to load RES into PPD-Lip to fabricate PPD-Lip@RES for alopecia treatment (Scheme 1). Firstly, RES has good antioxidant, anti-inflammatory activities and could restore the homeostasis of the hair follicle microenvironment, which provides good soil for cell proliferation and angiogenesis. Secondly, PPD-Lip itself has been confirmed that it could accelerate angiogenesis, reshape the hair follicle microcirculation system, and promote proliferation, migration, and gene expression of DPCs. Therefore, PPD-lip is expected to form a good complement with RES for alopecia therapy. Thirdly, the use of nanovesicles could increase the solubility, stability, and transdermal delivery and retention of RES, thereby significantly improving its anti-hair loss efficacy. All in all, different from most one-target drug development strategies for alopecia treatment, PPD-Lip@RES based on comprehensive strategy could exert the treatment effect on alopecia via multiple mechanisms and pathways, thereby has broad prospects.

Materials and Methods

Materials

Soybean lecithin was bought from A.V.T. Pharmaceutical Co., Ltd. (Shanghai, China). Protopanaxadiol was purchased from Nanjing Spring & Autumn Biological Engineering Co., Ltd. (Nanjing, China). Matrigel matrix was provided by Corning (USA). Nitric Oxide Assay Kit was obtained from Beyotime (Shanghai, China). IL-6 and TNF-α ELISA kits were purchased from Boster Biological Technology (Wuhan, China). Ki67 antibody (GB111499) was purchased from Servicebio Technology Co., Ltd (Wuhan, China). β- Catenin antibodies (51067-2-AP) and CD31 antibodies (28083-1-AP) were purchased from Proteintech. CK19 antibody (YT1269) was purchased from ImmunoWay Biotechnology. Cytokeratin 5 antibody (bs-1060R) was purchased from Biosynthesis Biotechnology Co., Ltd. (Beijing, China). DMEM

medium, Fetal Bovine Serum (FBS), and Phosphate Balanced Solution (PBS) buffer were purchased from Gibco (USA). 2',7'-dichlorofluorescein diacetate (DCFH-DA) was provided by MedChemExpress LLC (Shanghai, China). Minoxidil, resveratrol, and testosterone propionate came from Macklin Biochemical Co., Ltd. (Shanghai, China). The dialysis bag was bought from Viskase (USA). Animal hair removal cream was purchased from Nair (USA). Endothelial Cell Medium (ECM) was purchased from ScienCell (USA). Lipopolysaccharide (LPS), Iron (II) sulfate heptahydrate, salicylic acid, and DHE dye solutions were obtained from Sigma Aldrich (USA). Hydrogen peroxide(H_2O_2) was purchased from Guanghua Technology Co., Ltd. (Guangdong, China). Paraformaldehyde(4%,w/w) was bought from Yongjin Biotechnology Co., Ltd. (Guangzhou, China). Minoxidil tincture (5%,w/w)was purchased from Wansheng Pharmaceutical Co., Ltd. (Zhejiang, China).

Cell Lines and Animals

DPCs were purchased from BLUEFBIO Co., Ltd. (Shanghai, China), human umbilical vein endothelial cells (HUVECs), RAW264.7, and C57BL/6 mice (5 ~ 6 weeks old) were provided by the Laboratory Animal Center of Sun Yat-sen University (Guangzhou, China). The use of the cell lines was approved by the research ethics committee of Sun Yat-sen University. All the animal procedures were conducted according to the laboratory animal regulations approved by the Institutional Animal Care and Use Committee of Sun Yat-sen University, Ethics Approval No. 2022000828.

Preparation and Characterization of Nanovesicles

PPD-Lip@RES was prepared through the ethanol injection method. RES, PPD, and soybean lecithin were mixed at mass ratios of 1:1:3, 0.8:1:3, 0.4:1:3, and 0.2:1:3, slowly injected the mixture into deionized water using a micropipette gun under room temperature, and continue stirring for 30 min to obtain PPD-Lip@RES. PPD-Lip@MNX was prepared in the same way. The particle sizes and size distributions of nanovesicles were measured by Zetasizer Nano ZS90 (Malvern, U. K.). Additionally, transmission electron microscopy (TEM; JOEL, Japan) under 120 kV was employed to assess the morphological characteristics. Notably, the alterations of particle size and PDI under different dilutions and times at room temperature were used to evaluate the stability of the nanovesicles.

The drug concentrations of PPD-Lip@RES and PPD-Lip@MNX were analyzed via high-performance liquid chromatography (HPLC, Agilent, USA), using an XB-C18 column (Waters, 250 mm × 4.6 mm, 5 μm) with a mobile phase of acetonitrile/0.12% acetic acid water (65: 35, v/v), at a flow rate of 1.0 mL/min and a detection wavelength of 306 nm for RES, ZORBAX SB-C18 (Agilent, 250 mm × 4.6 mm, 5 μm) with a mobile phase of methanol/water (80: 20, v/v), at a flow rate of 1.0 mL/min and a detection wavelength of 230 nm for MNX. According to the previous method,[14] the drug loading (DL%) and encapsulation efficiency (EE%) were obtained according to the following equations:

$$EE\% = \left(1 - \frac{W_{Free}}{W_{Total}}\right) * 100\%$$

$$DL\% = \frac{(W_{Total} - W_{Free})}{(W_{Totallipids} + W_{Total} - W_{Free})} * 100\%$$

Where W_{Free}= drug content not encapsulated in liposome; W_{Total}= total drug content; $W_{total\ lipid}$= total lipid content.

In vitro Transdermal Experiment

The SD rat abdomen skin was excised, removed the adipose tissue, and fixed on the Franz diffusion cell with a permeation square of 3.14 cm^2 (TK-24BL, Kaikai Technology Co., Ltd., Shanghai, China), and 8 mL of normal saline with 40% PEG (v/v) served as the receiving medium, stirring at 250 rpm with a constant temperature of 32 ± 0.5°C. Subsequently, 0.5 mL PPD-Lip@RES or RES was added to the donor cell, which contained 25 μg of RES (n = 5). One milliliter of release medium was collected at 2 h, 4 h, 6 h, 8 h, 12 h, and 24 h, and an equal volume of medium was added to the receptor. The cumulative permeated amount of RES was evaluated by HPLC. Additionally, the skin retention of drugs was quantified.

The metabolism of RES and MNX in skin homogenate was also measured (see Supplementary Materials Experimental Section for details).

In vitro Pharmacodynamic Evaluation

Cell Proliferation Assay

DPCs were seeded in 96-well plates at a cell density of 2.5×10^3 cells per well. Upon adherence to the plate surface, the cells were subjected to treatment with 10 μM of MNX, RES, PPD-Lip@MNX, and PPD-Lip@RES. Subsequently, the cells were cultured for 24, 48, and 72 h, and the impact of different formulations on DPC proliferation was assessed using the CCK8 assay (ESscience, China). Similarly, HUVECs were seeded in 96-well plates at a density of 3×10^3 cells per well, using identical procedures to evaluate the effects of the various drugs on their proliferation. The cytotoxicity of different formulations on DPCs and HUVECs was measured via MTT assay (see Supplementary Materials Experimental Section for details).

Cell Migration Experiment

The influence of nanovesicles on cellular migration was assessed via scratch wound assay. Specifically, logarithmic-phase DPCs and HUVECs were seeded and cultured in a 6-well plate until approximately 80 ~ 90% confluence was reached. Next, a 200 μL pipette tip was used to draw the liner scratch on the cell monolayer, followed by rinsing with PBS. Subsequently, 2 mL of medium containing MNX, RES, PPD-Lip, PPD-Lip@MNX, and PPD-Lip@RES were introduced. The plate was incubated for 48 h, and the migration of the cells was observed at 0, 24, and 48 h using an inverted microscope. Quantification of the scratch area and healing rate was accomplished utilizing Image J software.

HUVECs Tubule Formation Experiment

Matrigel matrix was evenly coated on the surface of each well in a 96-well plate, utilizing a volume of 50 μL per well. Subsequently, the plate was incubated at 37°C for 30 min. Next, HUVECs suspension mixed with MNX, RES, PPD-Lip, PPD-Lip@MNX, and PPD-Lip@RES (n = 3), which contained 3×10^4 cells, were seeded to each well. After culturing for 4 h, the formation of tubes was observed under the microscope. The number of mesh circles per field was quantified by Image J.

Isolation and Treatment of Mice Vibrissa Follicles

According to the literature,[15] three-week-old male C57BL/6 mice were sacrificed, and the whisker pads were separated. The isolated vibrissa follicles were transferred to separate wells of a 48-well plate and incubated with the culture medium containing 10 μM of MNX, RES, PPD-Lip@MNX, PPD-Lip@RES (n = 5), and the control group supplemented with medium only. Follicles images were imaged every three days by the microscope, and the length of vibrissae follicles was quantified using Image J software. Additionally, morphological evaluation was conducted via hematoxylin and eosin (H&E) staining.

Mechanism Research

PCR Assay

According to the previous research method,[14] the expression levels of β-catenin, vascular endothelial growth factor (VEGF), insulin-like growth factor-1 (IGF-1), and matrix metalloproteinase 3 (MMP3) in DPCs were investigated through quantitative real-time polymerase chain reaction (qRT-PCR). The extraction of total cellular RNA from DPCs and reverse transcription was performed following the manufacturer's protocols. The data were normalized to the level of GAPDH. The primer sequences employed for this investigation could be found in Table 1.

Antioxidant Activity Evaluation

According to the experimental method proposed by Zhang et al,[16] we evaluated the in vitro antioxidant activity of MNX, RES, PPD-Lip, and PPD-Lip@RES by examining their scavenging ability of DPPH, ·OH, and ABTS radicals.

Table 1 DNA Sequence of Primer Pairs Used for qRT-PCR in DPCs

Gene	Forward Primer	Reverse Primer
GAPDH	TGAAGGTCGGAGTCAACGG	TGGAAGATGGTGATGGGAT
β-catenin	CATCTACACAGTTTGATGCTGCT	GCAGTTTTGTCAGTTCAGGGA
VEGF	AGGGCAGAATCATCACGAAGT	AGGGTCTCGATTGGATGGCA
IGF-1	GCTCTTCAGTTCGTGTGTGGA	GCCTCCTTAGATCACAGCTCC
MMP3	AGTCTTCCAATCCTACTGTTGCT	TCCCCGTCACCTCCAATCC

Protective Effect of Drugs on H_2O_2-Damaged Cells

To investigate the protective effect of drugs on H_2O_2-damaged cells, DPCs were seeded into 96-well culture plates at a density of 2.5×10^3 cells each well and added 200 μM of H_2O_2 to induce oxidative damage cell model. Furthermore, 10 μM or 20 μM of RES and PPD-Lip@RES were added, and the cell viability was measured by MTT assay after 24 h of cultivation.

Clearing Effect of Drugs on Intracellular ROS

The assessment of drug-induced clearance of intracellular ROS was conducted by evaluating the fluorescence intensity of intracellular DCF. Briefly, the DPCs were cultured in glass dishes at a density of 2×10^5 cells/well. After attachment, the cells were incubated with 10 μM or 20 μM of RES and PPD-Lip@RES and exposed to H_2O_2 (200 μM) (n = 6). The DMEM-only group was used as blank control and the H_2O_2-only group served as a negative control. After 24 h of incubation, the DCFH-DA probe staining (10 μM) was then added and the cells were further incubated for 20 min, while the DAPI was used for cell nucleus staining. Subsequently, the fluorescence intensity of intracellular DCF was visualized under laser scanning confocal microscope (CLSM; Olympus, Japan).

In vitro Anti-Inflammatory Activity

RAW264.7 cells were seeded into a 96-well plate at a 1.5×10^4 cells/well density. Except for the control group, other groups were stimulated with LPS (2 μg/mL). The DMEM-only group was used as blank control, and the LPS-only group served as a negative control. The drug treatment groups were also incubated with MNX, RES, PPD-Lip, PPD-Lip@MNX, and PPD-Lip @RES, respectively. After culturing for 24 h, cellular morphology was observed and recorded by microscope. Meanwhile, the content of NO, IL-6, and TNF-α in cell supernatant from each group was detected utilizing ELISA Kits.

Pharmacodynamical Studies

Telegen Effluvium (TE) Model

Based on the previous research method,[14] the TE model was established. Seven-week-old C57BL/6 mice were randomly divided into 5 groups (n = 5). Following anesthesia, the dorsal hair of the mice was shaved, and depilatory cream was utilized to ensure complete hair removal. After recovering for one day, the mice were topically treated with 0.2 mL of different formulations: normal saline, MNX tincture (5 mg/mL MNX), PPD-Lip@MNX (contained 5 mg/mL MNX), or PPD-Lip @RES (contained 5 mg/mL RES). To evaluate body weight, changes in dorsal skin color, and hair regrowth, photographs of the mice in each group were captured on day 6, 9, 12, 15, and 30. At the end of the experiment, the mice were anesthetized, and a "hair pull test" was conducted using transparent tape to record the extent of hair loss. Subsequently, the regeneration hair of mice was collected and weighed, and the morphological characterization was observed by Field Emission Scanning Electron Microscope (FESEM; JOEL, Japan) and inverted microscope, and the diameter of the hair shaft was measured by Image J.

AGA Model

Based on the previous research method,[14] the severe AGA model was established by subcutaneous injection of 0.2 mL of testosterone propionate (TTP, 5 mg/mL) once daily for continuous 20 days. Briefly, the mice were randomly classified into five groups (n = 5), wherein the blank control group and model group received topical application of normal saline, while other groups topical application of 0.25% finasteride (FIN), RES (5 mg/mL), and PPD-Lip@RES (containing 5 mg/mL of RES). Subsequently, photographs of the mice in each group were captured on day 0, 15, 25, 30, 40, 50, 60,

65, and 70, and the same evaluations were performed as the TE model. Image J software was employed to calculate the hair coverage of mice in each group from day 60 to day 70. Concurrently, a hair detection device was utilized to assess hair regeneration in each group. To further investigate the stage of hair follicle cycle after hair regeneration in each group, the dorsal skin color was observed after shaving new hair.

Histological Analysis, Immunofluorescence Staining, and Immunohistochemical Experiments

Upon isolation of the dorsal skin, fixed with paraformaldehyde, followed by H&E and Masson staining for hair follicles and skin morphologies observation. The skin thickness and hair bulb diameter were measured by Image J, and hair follicle cycling was analyzed based on established hair follicle morphological criteria.[17] Additionally, the oxidative state of the dorsal skin in severe AGA mice was evaluated through DHE staining. To evaluate the hair follicle cell proliferation in each group, Ki67 and keratin 5 (K5) immunofluorescence staining was applied to paraffin-sectioned dorsal skin samples. Furthermore, β-catenin immunofluorescence mono staining was employed to scrutinize the expression of β-catenin in skin tissues. Finally, immunohistochemistry analysis was conducted to examine the expression of CD31 and CK19 in each group.

The mRNA expression levels of β-catenin, VEGF, Wnt3a, fibroblast growth factors-5 (FGF-5), bone morphogenetic proteins (BMP2), dickopff-1 (DKK-1), and transforming growth factor-1 (TGF-β1) on the dorsal skin of mice in each group were detected by quantitative real-time PCR analysis. The primer sequences utilized can be found in Table S1 (see Supplementary Materials Experimental Section for details).

Statistical Analysis

All data were presented as means ± standard deviation. The statistical evaluation of significant differences was performed by one-way analysis of variance (ANOVA) followed by Tukey's multiple comparison test with GraphPad Prism version 9 software.

Results and Discussion

Preparation and Characterization of Nanovesicles

As shown in Table S2, the encapsulation efficiency of PPD-Lip@RES was higher than 80% under different RES dosages from 4.8% to 20.0%, indicating that PPD-Lip@RES possesses high drug loading to meet the actual need in clinical. Similarly, the encapsulation efficiency of PPD-Lip@MNX was 87% (Table S3). The PPD-Lip@RES exhibited a particle size of approximately 120 nm, a zeta potential of approximately −12.6 mV (Table S4), and the PPD-Lip@MNX had a particle size of about 150 nm with uniform dispersion, zeta potential of about −10.8 mV (Table S5).

As shown in Figure 1a–d, the TEM results showed that PPD-Lip@RES and PPD-Lip@MNX were spherical in shape, with particle sizes of 115.39 ± 8.27 nm and 143.94 ± 7.82 nm, respectively. PPD-Lip@RES and PPD-Lip@MNX have good dilution and placement stability. When diluted to 100-fold and placed for 30 d, the particle size and PDI have no obvious change, and no obvious aggregation was observed.

The in vitro transdermal experiment results showed that at 24 h after treatment, the cumulative permeation of RES and PPD-Lip@RES was 786.53 ± 180.93 μg and 442.38 ± 137.47 μg, respectively. Skin retention was 95.20 ± 13.69 μg/cm^2 and 54.99 ± 13.39 μg/cm^2, respectively (Figure 1e and f), indicating that PPD-Lip@RES could significantly improve the skin penetration and retention of RES.

As shown in Figure 1g and h, the cumulative permeation of MNX in the free MNX group (487.90 ± 122.68 μg) was higher than that in the PPD-Lip@MNX group (390.42 ± 64.55 μg). Because MNX was a highly permeable drug with good transdermal properties,[11] the cumulative permeability of free MNX was slightly higher than that of the nanovesicle group. The skin retention of MNX in PPD-Lip@MNX group (23.67 ± 4.85 μg/cm^2) was significantly higher than that in free MNX group (14.53 ± 5.15 μg/cm^2), indicating that PPD-Lip@MNX could increase the skin retention of MNX.

In vitro Promote DPCs Proliferation, Migration, and Regulate Gene Expression

Dermal papilla (DP) serves as the signaling center for hair follicles, and its primary component, known as DPCs, plays a crucial role in regulating the regeneration and cycle of hair follicles by stimulating epithelial HFSCs. In addition, DPCs

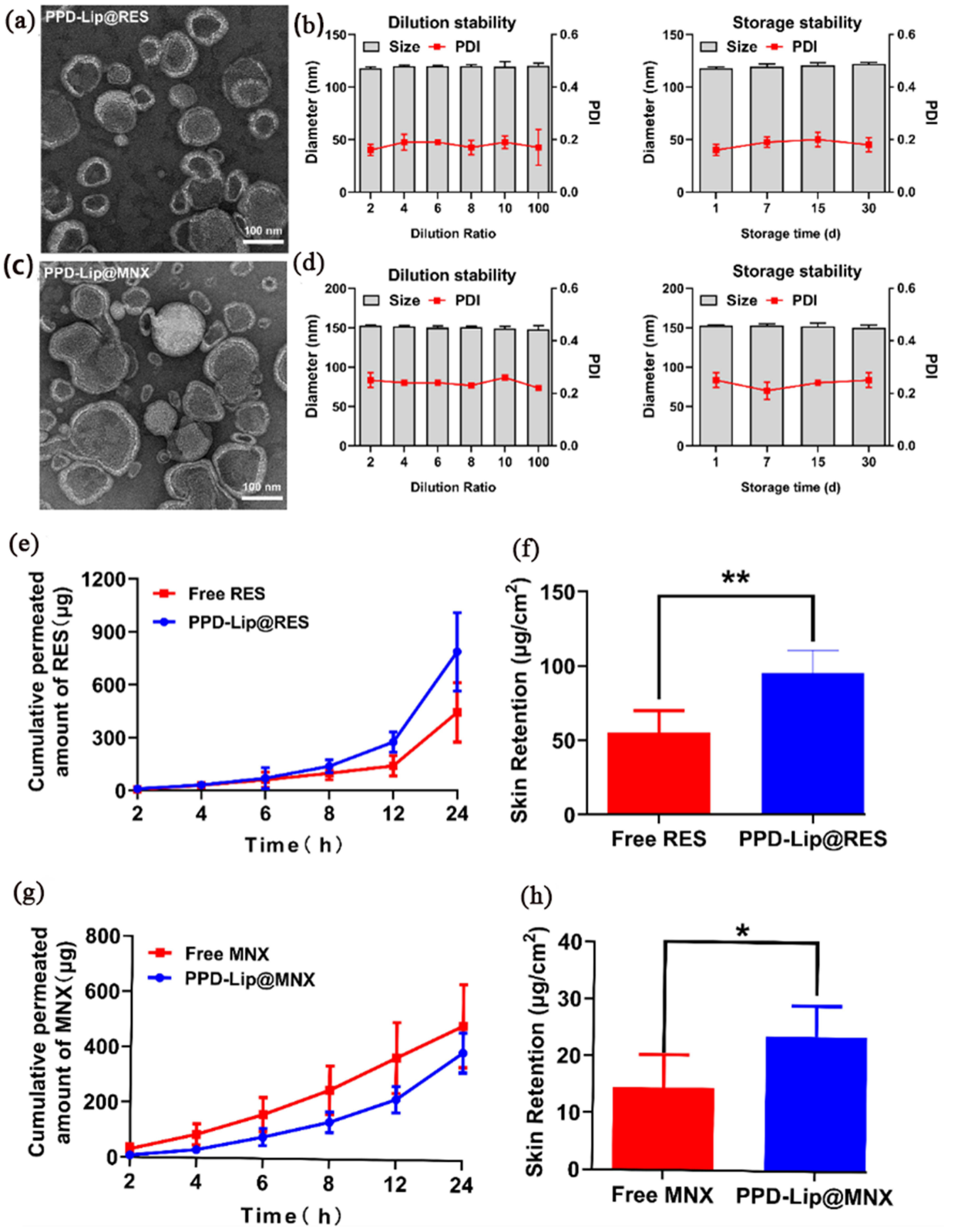

Figure 1 TEM image and stability of PPD-Lip@RES (**a** and **b**) and PPD-Lip@MNX (**c** and **d**). In vitro transdermal experiments with different formulations: Cumulated permeation and skin retention of RES (**e** and **f**) or MNX (**g** and **h**). *$P < 0.05$ vs Free MNX, **$P < 0.01$ vs Free RES. The skin contains a large number of enzymes, which could decompose drugs when they penetrate through the skin, and thus impeding the arrival of drugs at the target site.[18] Therefore, it was significant to investigate the metabolic behavior of drugs in the skin. The skin homogenate obtained from homogenized mouse skin tissue could preserve the enzyme system in the skin. The concentration of RES, varying from 98% to 105%, RSD < 2% at 24 h after incubation with skin homogenate, indicating RES was not easily metabolized by enzymes in the skin and could exist stably in the skin, which was conducive to exert drug efficacy. Similarly, the concentration of MNX varies between 99% and 101%, showing good stability (Figure S1).

proliferate during the growth phase and could secrete various signaling factors, which contribute to hair regeneration.[19] Thus, DPCs have become a critical cellular model for studying the effects of hair growth regulators on hair follicles.[19] We investigated the effects of different formulations on DPCs. First, the cytotoxicity of MNX, PPD-Lip@MNX, RES, and PPD-Lip@RES to DPCs at different concentrations was investigated by MTT assay. The results showed that the cell viability in each group was more than 80% at a concentration of 50 μM, indicating good cell safety of drugs (Figure S2). When the drug concentration was 10 μM, the cell viability of MNX, PPD-Lip@MNX, RES, and PPD-Lip@RES groups were 105.02 ± 6.71%, 125.12 ± 6.83%, 114.58 ± 8.82%, and 143.85 ± 5.62%, respectively. The results indicated that the effect of RES on DPCs proliferation was superior to MNX at 10 μM. According to the literature,[14] MNX at the concentration of 10 μM serves as positive control.

As shown in Figure 2a, with the prolongation of drug administration, the cell proliferation rate gradually increased, among which, PPD-Lip@RES has the strongest proliferative effect on DPCs, with a cell proliferation rate of 163.59 ± 16.87% after 72 h of treatment. The proliferative rates of MNX, RES, and PPD-Lip@MNX were 116.66 ± 5.73%, 122.04 ± 6.36%, and 145.60 ± 6.38%, respectively, indicating that loading MNX and RES into PPD-Lip could superimpose the proliferative effects of drugs and carriers on DPCs. Moreover, since RES has a stronger proliferative effect on DPCs than MNX, the effect of PPD-Lip@RES was stronger than that of PPD-Lip@MNX.

The results of the DPC migration experiment were displayed in Figure 2b and c, the scratch area of cells in all groups decreased gradually with the extension of time, and the scratch area of cells in PPD-Lip, PPD-Lip@MNX, and PPD-Lip @RES groups were completely closed after 48 h. The relative cell mobility of MNX and RES groups was 54.76 ± 0.19% and 70.00 ± 1.50%, respectively (Figure 2b), indicating that the ability of promoting cell migration was weak in the free drug groups. After loading the drugs into the active vehicle, PPD-Lip could enhance the role of RES in promoting cell migration, thereby facilitating hair regeneration.

Furthermore, in order to explore the regulatory effect of drugs on the expression of hair growth-related genes in DPCs, the expressions of β-catenin, VEGF, IGF-1, and MMP3 in DPCs after treatment were investigated by PCR. Wnt/β-catenin signaling pathway was one of the key pathways controlling hair growth and cycle,[20] and it plays a vital role in maintaining hair follicle growth and development, stem cell aggregation, and differentiation. β-catenin was the core effector of the Wnt/β-catenin signaling pathway. Activation or upregulation of β-catenin was essential for promoting hair growth, which could facilitate the transition of hair follicles from the telogen phase to the anagen phase. The formation of blood vessels around hair follicles played an essential role in the periodic circulation of hair follicles and hair growth.[21] VEGF, as a growth factor, exerts stimulatory effects on angiogenesis, and its overexpression was associated with enhanced angiogenic activity. In addition, MMP3 and IGF-1 were essential regulators of hair follicle growth. MMP3 could affect adult epithelial stem cells by activating the Wnt/β-catenin signaling pathway, thereby stimulating hair follicle growth.[20] IGF-1 could promote the proliferation and migration of hair follicle cells, reduce cell apoptosis, promote the hair follicle to enter the growth phase, and delay the degeneration phase, which was essential for maintaining the hair growth phase and extending the hair shaft length.[22]

As shown in Figure 2d - g, in comparison to the untreated negative control, the drug treatment groups exhibited up-regulated expressions of β-catenin, VEGF, IGF-1, and MMP3, and PPD-Lip@RES had the strongest up-regulation effect ($P < 0.05$). These results indicated that PPD-Lip@RES could promote the hair follicles to enter the anagen phase and maintain the continuous growth of hair by activating the Wnt/β-catenin signaling pathway, stimulating angiogenesis, promoting the proliferation and migration of hair follicle cells and other mechanisms.

In vitro Promote HUVECs Proliferation, Migration, and Angiogenesis

Adequate blood supply could transport abundant nutrients and bioactive molecules such as growth factors, to hair follicles, which was crucial for meeting the high metabolic energy need and the maintenance of hair follicles during growth.[23] Studies had shown that the density and volume of blood vessels around hair follicles were the largest in the anagen phase and gradually decrease or disappear in the catagen and telogen phases. The formation of blood vessels was positively correlated with the diameter of the hair shaft and hair bulb.[21] Degeneration of blood vessels around hair follicles and disorder of hair follicle microcirculation could promote hair follicles entering the catagen and telogen phase, leading to hair loss. Androgen receptor-mediated parasecretory signals in DPCs of AGA patients could lead to apoptosis

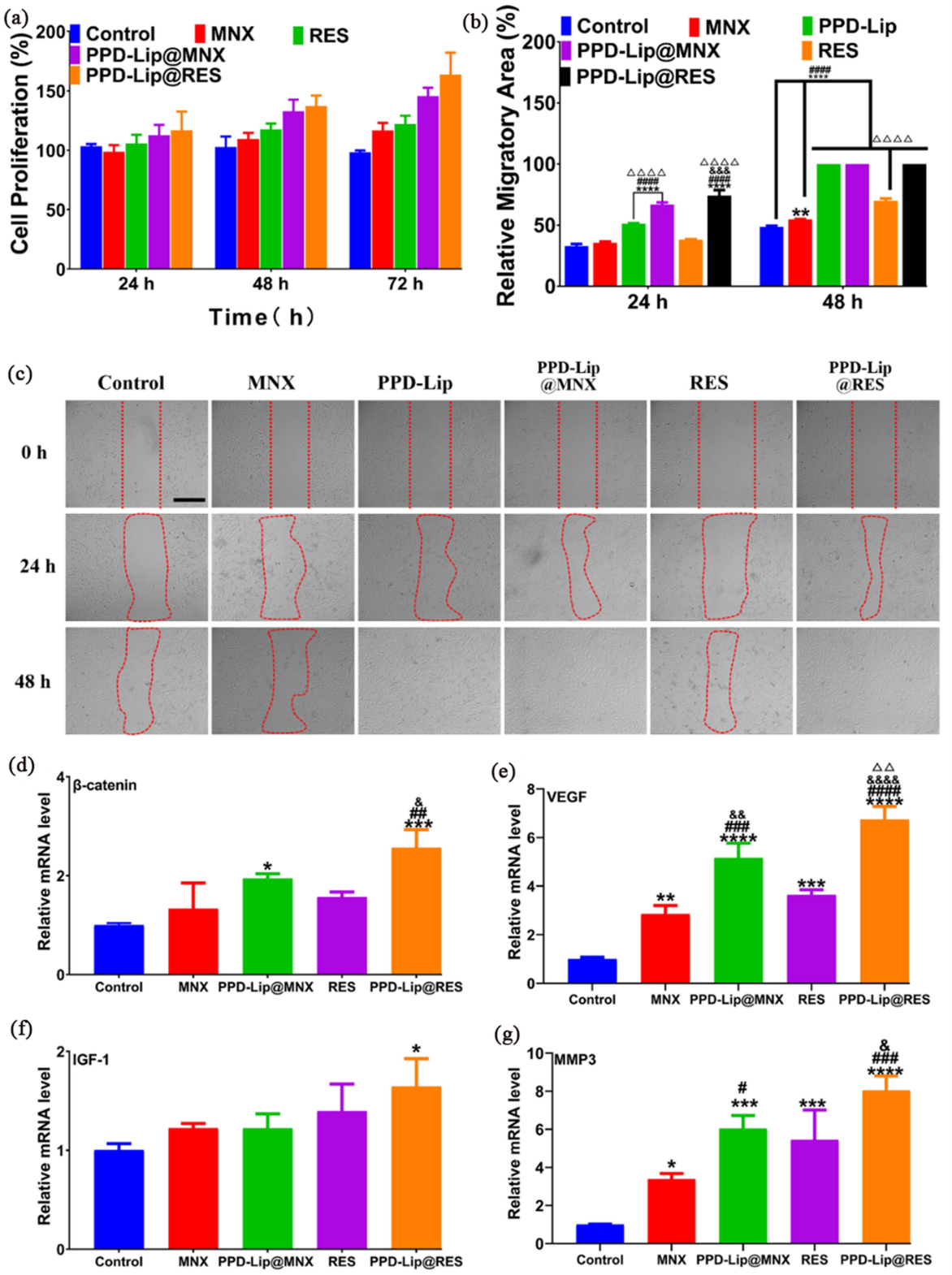

Figure 2 (**a**) Cell proliferation of DPCs after treated with different formulations. (**b**) Quantitative analysis of the migration rate of DPCs in Figure 2c. $^{**}P < 0.01$; $^{****}P < 0.0001$ vs Control; $^{\#\#\#\#}P < 0.0001$ vs MNX; $^{\&\&\&}P < 0.001$ vs PPD-Lip@MNX. $^{\triangle\triangle\triangle\triangle}P < 0.0001$ vs RES. (**c**) Representative images of DPCs migration, scale bar = 400 μm. The mRNA expression levels of β-catenin (**d**), VEGF (**e**), IGF-1 (**f**), MMP3 (**g**) in DPCs. $^{*}P < 0.05$; $^{**}P < 0.01$; $^{***}P < 0.001$; $^{****}P < 0.0001$ vs Control. $^{\#}P < 0.05$; $^{\#\#}P < 0.01$; $^{\#\#\#}P < 0.001$ vs MNX. $^{\&}P < 0.05$; $^{\&\&}P < 0.01$; $^{\&\&\&\&}P < 0.0001$ vs RES; $^{\triangle\triangle}P < 0.01$ vs PPD-Lip@MNX.

of microvascular endothelial cells around DP, eventually leading to a degeneration of peri-follicle vessels and miniaturization of hair follicles.[24] Therefore, promoting the proliferation of vascular endothelial cells, enhancing vascularization around hair follicles, and reshaping microcirculation to meet the nutritional need of hair growth were crucial for hair regeneration.

The cytotoxicity results of MNX, PPD-Lip@MNX, RES, and PPD-Lip@RES on HUVECs at different concentrations were shown in Figure S3. At the concentration of 50 μM, the RES group exhibited certain toxicity to cells (viability 61.71 ± 2.54%). And the toxicity absolutely was attributed to the solvent, 0.5% ethanol, which was used to increase the solubility of RES. Comparatively, at the same concentration of 50 μM, the cell viability of PPD-Lip@RES was 102.53 ± 11.55%, indicating that loading RES into nanovesicles could not only effectively increase RES's solubility but also eliminate the toxicity derived from the solvent. When the drug concentration reduced to 10 μM, the cell survival rates of MNX, PPD-Lip @MNX, RES, and PPD-Lip@RES groups were 103.21 ± 7.41%, 129.86 ± 6.08%, 114.22 ± 5.49%, and 138.05 ± 7.44%, respectively, indicating that PPD-Lip@RES had a good effect on promoting the proliferation of HUVECs.

The proliferation rate of HUVECs cells increased in a time-dependent manner. At 72 h, the cell proliferation rates of MNX, PPD-Lip@MNX, RES, and PPD-Lip@RES were 119.77 ± 4.18%, 132.77 ± 5.00%, 123.41 ± 4.92%, and 159.03 ± 23.95%, respectively (Figure 3a), indicating that PPD-Lip could promote HUVECs proliferation of drugs, and the effect of PPD-Lip @RES was superior to PPD-Lip@MNX.

The effects of different formulations on HUVECs migration were shown in Figure 3b, the scratch area of cells in all groups decreased gradually with the extension of time, and the scratch area of cells in PPD-Lip@RES group was completely closed after 48 h. By contrast, the scratch area of cells in MNX, PPD-Lip, PPD-Lip@MNX, and RES groups did not completely heal at 48 h, and the migration rates were 59.03 ± 2.29%, 70.59 ± 10.23%, 82.43 ± 4.39%, and 99.44 ± 0.96%, respectively (Figure 3c). PPD-Lip@MNX demonstrated a favorable effect in promoting cell migration, which attribute to the promotion effect of PPD-Lip itself on the migration of HUVECs. It's noteworthy that PPD-Lip@RES was superimposed with the dual effects of RES and PPD-Lip, which had the strongest effect of promoting HUVECs migration, with the cell migration rate reaching 97% after 24 h of treatment.

The in vitro tube formation experiment results showed that compared with the control group, more tubes were formed on the matrix gel at 4 h after treatment in the drug groups (Figure 3d and e). Among them, RES had a significantly stronger ability to promote angiogenesis in vitro than that of MNX ($P < 0.001$). Coupled with the carrier's own angiogenic effect, the PPD-Lip@RES group showed the strongest angiogenic ability, which was expected to reshape hair follicle blood vessels, improve hair follicle microcirculation, and restore blood supply to the hair follicle microenvironment to meet the nutritional need of hair follicles, drive hair follicles into the anagen phase and maintain the anagen phase in vivo.

Promoted Vibrissae Hair Shaft Elongation in Mouse Vibrissa HF Organ Model

The growth of mouse hair follicles in vitro was strongly related to the growth of hair in vivo.[25] The mice vibrissa follicle was a typical model for evaluating the effect of drugs on hair follicle growth. Generally, mouse vibrissa follicles begin to degrade and stop growing after a few days of in vitro culture without drug treatment. Therefore, the effect of drugs on hair follicles could be evaluated by comparing the elongation of mouse vibrissa follicles and the morphological characteristics of hair follicles after treatment with different drugs.

As shown in Figure 4a and b, after 12 d in vitro cultivation of mice vibrissa follicle, the cumulative hair shaft elongation of vibrissae in treatment groups was longer than that of the untreated control group. Among them, RES had a superior effect on promoting the growth of mice vibrissa follicles than MNX, and the PPD-Lip@RES group had the strongest effect in promoting hair shaft elongation ($P < 0.01$). The results showed that PPD-Lip@RES could promote the growth of hair follicles and the elongation of hair follicles in mice, which might attribute to the dual effects of RES and PPD-Lip.

H&E staining was used to investigate the morphology of mouse vibrissae follicles in each group. As shown in Figure 4c, DP of control group atrophied and moved upward, the hair bulb atrophy into rod-shaped, and the hair follicle was in the catagen stage. In the drug treatment groups, DP was spherical, and hair follicles were in the anagen stage. Among them, the RES and PPD-Lip@RES groups had larger diameters of hair bulbs, and had a better effect on

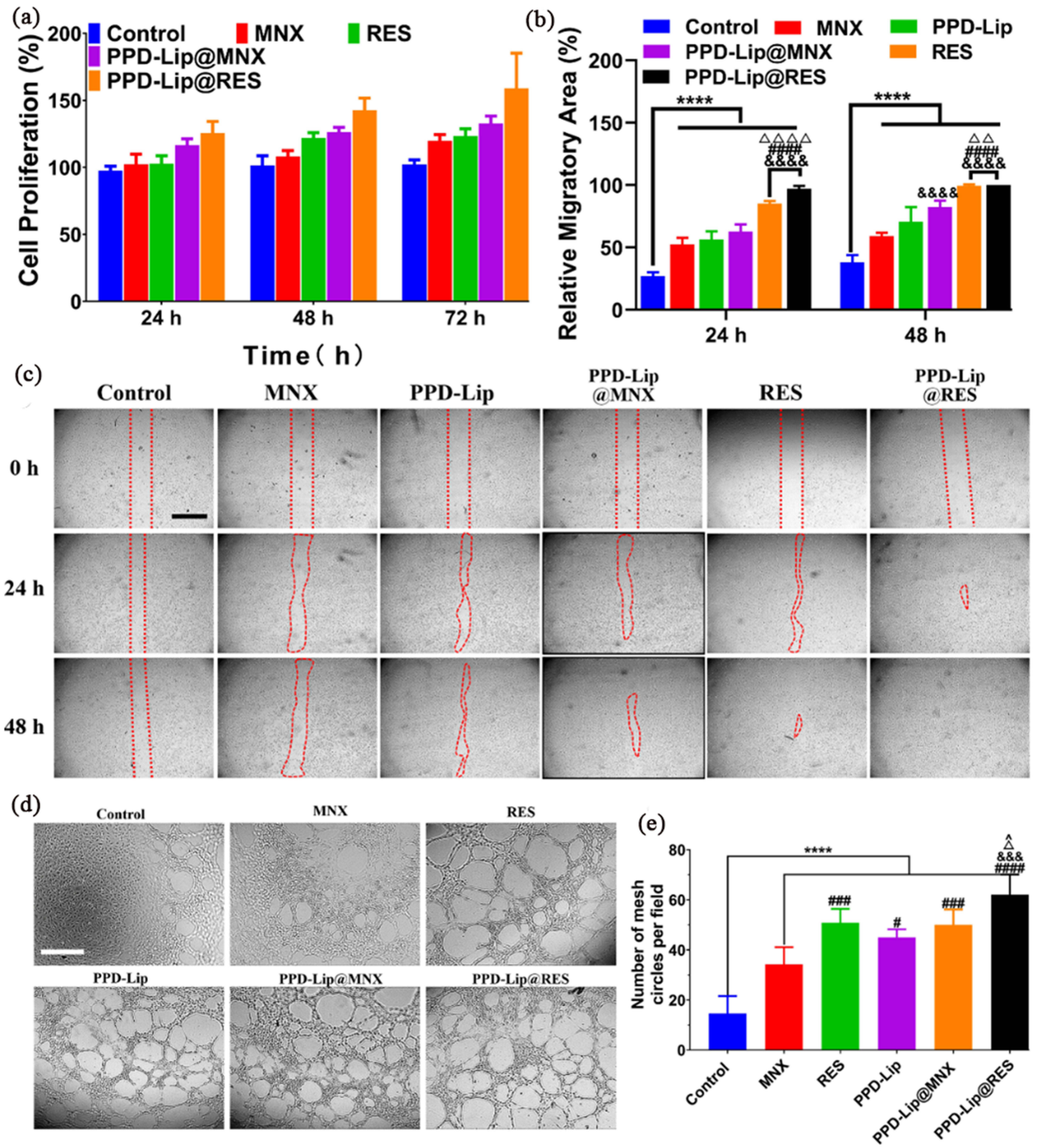

Figure 3 (**a**) Cell proliferation of HUVECs after treated with different formulations. (**b**) Quantitative analysis of the migration rate of HUVECs. $^{****}P < 0.0001$ vs Control; $^{\&\&\&\&}P < 0.0001$ vs MNX; $^{\#\#\#\#}P < 0.0001$ vs PPD-Lip. $^{\triangle\triangle}P < 0.01$, $^{\triangle\triangle\triangle\triangle}P < 0.0001$ vs PPD-Lip@MNX. (**c**) Representative images of the HUVECs migration, scale bar = 1000 μm. (**d**) Representative images of tube formation after treated with different formulations for 4 h, scale bar = 400 μm. (**e**) Quantitative analysis of the number of mesh circles in each field. $^{****}P < 0.0001$ vs Control. $^{\#}P < 0.05$; $^{\#\#\#}P < 0.001$ vs MNX. $^{\&\&\&}P < 0.001$ vs PPD-Lip. $^{\triangle}P < 0.05$ vs PPD-Lip@MNX. $^{\wedge}P < 0.05$ vs RES.

promoting the growth of mouse vibrissae follicles. These results indicated that RES and PPD-Lip@RES could promote the growth of mice vibrissae follicles and maintain the anagen phase of hair follicles in vitro. These results were in accordance with their promoting effects on the proliferation and migration of DPCs.

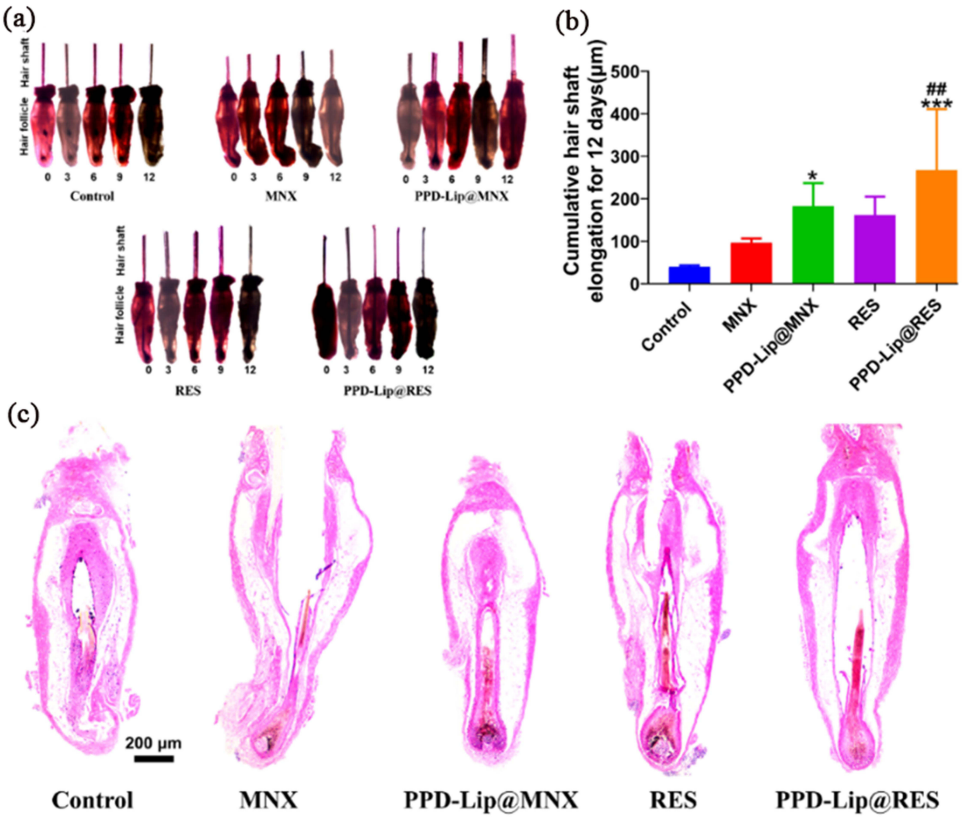

Figure 4 Different formulations accelerated vibrissae follicle growth in vitro. (**a**) Photographs of mouse vibrissa follicles culture for 0, 3, 6, 9 and 12 day. (**b**) Cumulative hair shaft elongation for 12 d. $^{*}P < 0.05$; $^{***}P < 0.001$ vs Control. $^{\#\#}P < 0.001$ vs MNX. (**c**) Representative H&E was staining images of vibrissae follicles at 12 day.

Antioxidant and Anti-Inflammatory Effects in vitro

Oxidative stress was involved in the development of AGA.[26] Studies had found that ROS levels in AGA patients were higher than those in the control group, and DPCs in the bald area were more sensitive to oxidative stress than those in non-balding areas. In addition, increased ROS levels were associated with inflammation, which increased the production of pro-inflammatory cytokines, resulted in damage to DNA, proteins, and lipid in the hair follicle environment.[27] Moreover, ROS could increase the secretion of hair growth inhibitor TGF β1 and induce DPCs senescence.[28] Therefore, the antioxidant significantly protects DPCs cells, maintains hair follicle microenvironment homeostasis, and promotes hair growth.

The antioxidant activity of PPD-Lip@RES was investigated by free radical scavenging experiments and intracellular antioxidant experiments. As shown in Figure 5a, MNX and PPD-Lip exhibited low clearance rate (20%) to DPPH even if the concentrations come up to 200 μM. In comparison, for RES and PPD-Lip@RES, removing 20% of DPPH only needed a concentration of 0.5 μM, and the DPPH scavenging effect showed a concentration dependent. The scavenging effect of RES and PPD-Lip@RES on DPPH was equivalent to that of vitamin C (Vc) at almost each concentration, indicating the excellent antioxidant activity of RES and PPD-Lip@RES. Moreover, the scavenging ability of RES and PPD-Lip@RES to ·OH and ABTS was much higher than that of Vc, while MNX and PPD-Lip showed weak activity even at 200 μM (Figure 5b and c). The results indicated that the antioxidant activity of PPD-Lip@RES was attributed to RES itself. The antioxidant capacity of PPD-Lip@RES makes it helpful to reduce the damage caused by oxidative stress occurring in hair follicles.

According to the literature,[29] H_2O_2 accumulates in human hair follicles. As a potent oxidizing agent, H_2O_2 could easily enter the cell membrane and generate highly reactive free radicals intracellularly. This process stimulated the production of ROS, which subsequently triggers oxidative damage and apoptosis. Furthermore, we used H_2O_2 as an oxidative damage inducer for DPCs to investigate the protective effect of RES and PPD-Lip@RES on DPCs. The

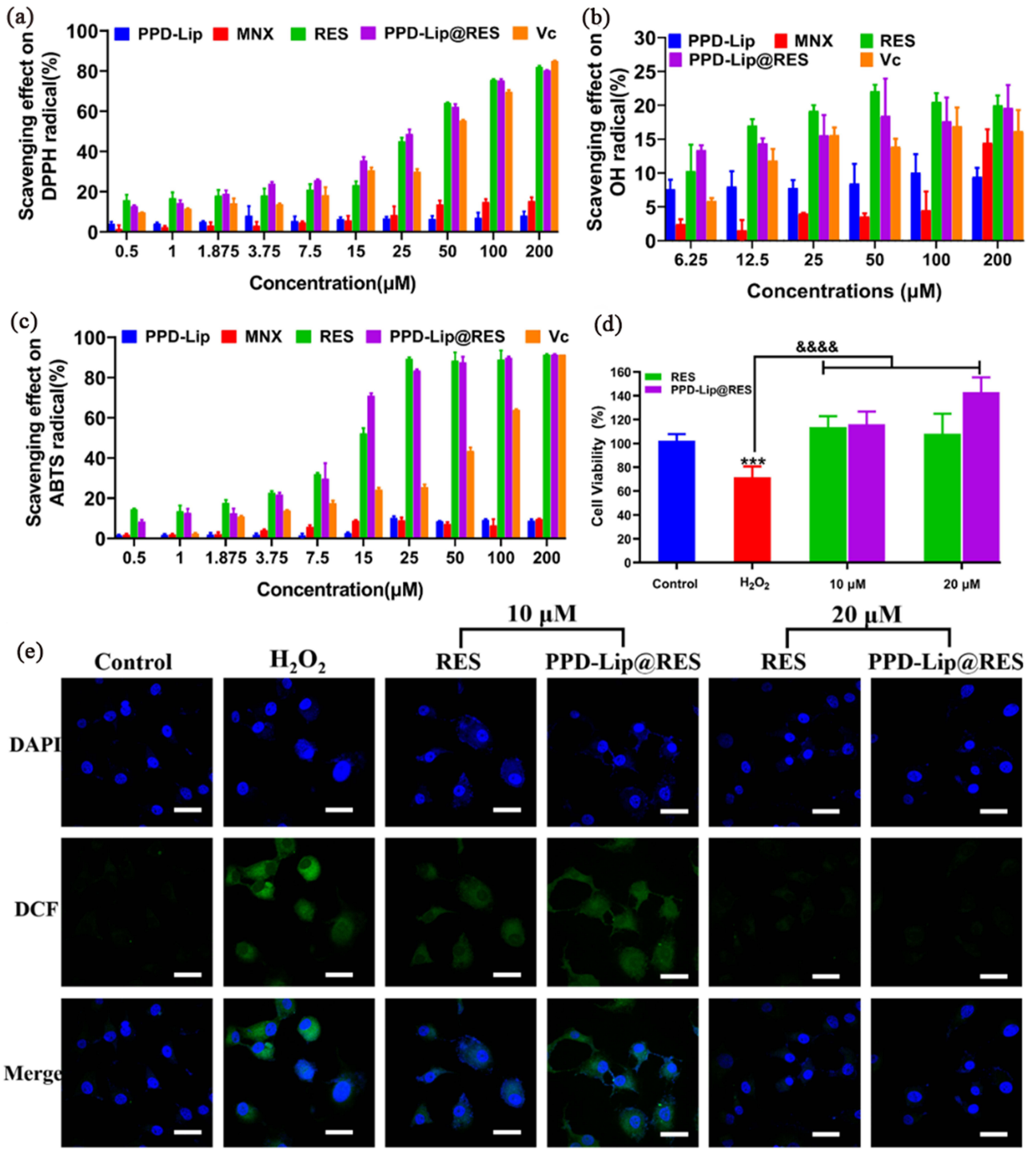

Figure 5 Ability of various formulations to scavenge DPPH (**a**), ·OH (**b**), ABTS radicals (**c**). (**d**) The protective effect of RES and PPD-Lip@RES in H_2O_2-induced DPCs cell damage. ***$P < 0.001$ vs Control. $^{\&\&\&\&}P < 0.0001$ vs H_2O_2. (**e**) RES reduces the intracellular ROS level of DPCs induced by H_2O_2.

modeling concentration of DPCs damaged by H_2O_2 was first explored here. As shown in Figure S4, the cell viability of DPCs decreased with the increase in H_2O_2 concentration. After 24 h treatment with 200 μM of H_2O_2, the cell viability was 74.6 ± 6.1%, significantly lower than that of the control group ($P < 0.001$). Therefore, 200 μM of H_2O_2 was chosen to construct the DPCs oxidative damage model.

As shown in Figure 5d, the cell viability of H_2O_2 group was 71.7 ± 7.7%, and the cell viability was significantly improved by RES and PPD-Lip@RES. At 10 μM, the cell viability of the RES group and PPD-Lip@RES group were 108.1 ± 13.4% and 116.1 ± 9.5%, respectively. When the concentration of RES reached 20 μM, the cell viability reached 113.7 ± 8.0% and 143.2 ± 10.3%, respectively. The result suggesting that RES and PPD-Lip@RES could protect DPCs from oxidative damage caused by H_2O_2 and promote the proliferation of DPCs.

DCFH-DA served as a widely employed probe for detecting ROS and did not have fluorescence. Upon entering the cell, it could generate non-fluorescent DCFH. When intracellular ROS was present, DCFH could be oxidized into fluorescent DCF, and observing the fluorescence intensity of intracellular DCF through CLSM could indirectly determine the ability to clear intracellular ROS.

As shown in Figure 5e, no DCF fluorescence was detected in the blank control group, while the H_2O_2 group showed strong green fluorescence. After drug treatment, the fluorescence intensity decreased with the increase in drug concentration. When the drug concentration reached 20 μM, the intracellular ROS level was basically consistent with the blank group, indicating that RES and PPD-Lip@RES could markedly clear intracellular ROS. The above results suggested that PPD-Lip@RES could relieve intracellular oxidative stress state by clearing free radicals and reducing intracellular ROS levels.

Inflammation was another important cause of hair loss, and studies had shown that some inflammatory cytokines negatively regulate HFSCs,[30] which could lead to hair follicle degeneration. NO, TNF-α and IL-6 could cause micro-inflammation of hair follicles, thereby hindering hair growth. Therefore, effectively inhibiting the release of these pro-inflammatory factors was of great significance for the prevention and treatment of hair loss. As shown in Figure 6a, after LPS stimulation, RAW264.7 cells transformed from a spherical shape to an irregular spindle shape, with pseudopodia stretching out, indicating the successful construction of a cellular inflammation model. After drug treatment, the number of deformed cells was significantly reduced, and the cell morphology of RES and PPD-Lip@RES groups had no

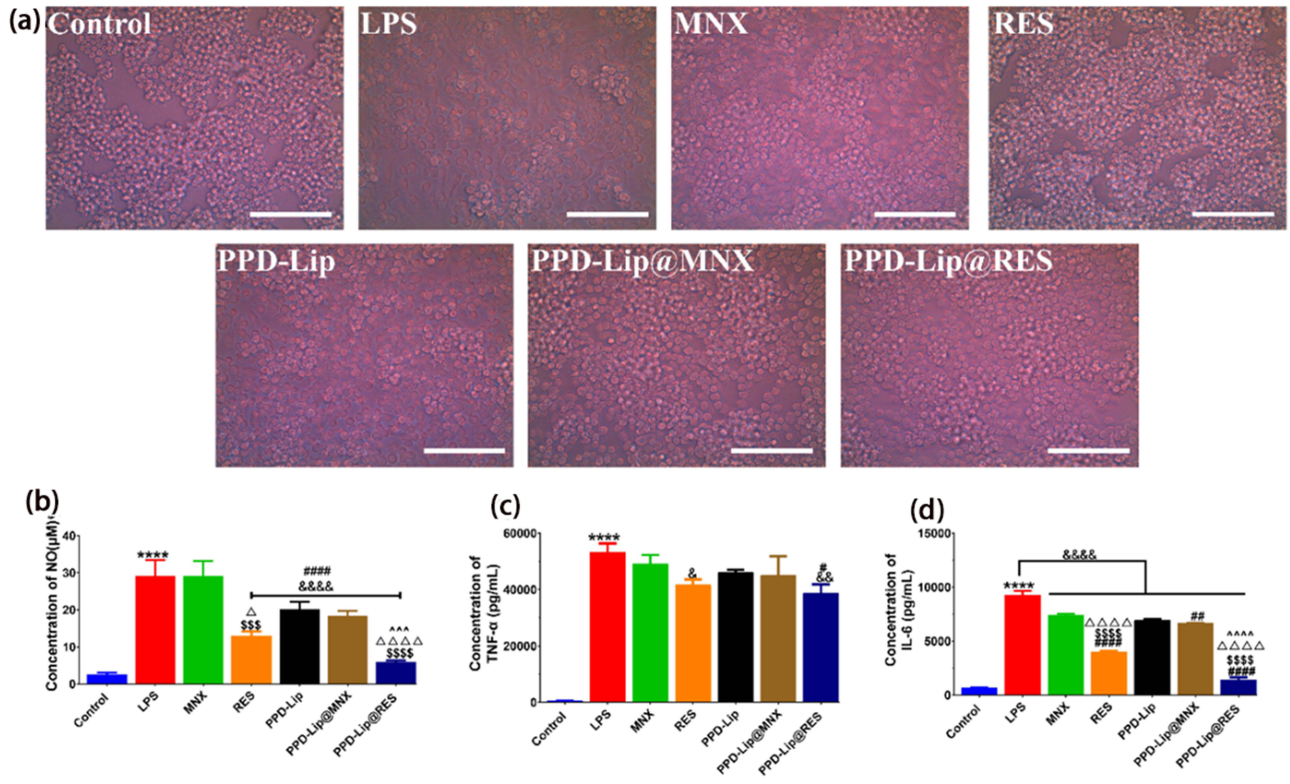

Figure 6 (**a**) Morphological of RAW264.7 in different groups. Scale bar =100 μm. The ability of different formulations to inhibit the production of inflammatory cytokines: (**b**) NO, (**c**) TNF-α, (**d**) IL-6. $^{****}P < 0.0001$ vs Control; $^{\&}P < 0.05$; $^{\&\&}P < 0.01$; $^{\&\&\&}P < 0.001$; $^{\&\&\&\&}P < 0.0001$ vs LPS. $^{\#}P < 0.05$; $^{\#\#}P < 0.01$; $^{\#\#\#\#}P < 0.0001$ vs MNX. $^{\$\$\$}P < 0.001$; $^{\$\$\$\$}P < 0.0001$ vs PPD-Lip. $^{\Delta}P < 0.05$; $^{\Delta\Delta\Delta\Delta}P < 0.0001$ vs PPD-Lip@MNX. $^{\wedge\wedge\wedge}P < 0.001$; $^{\wedge\wedge\wedge\wedge}P < 0.0001$ vs RES.

significant difference with the control group, indicating that they had good anti-inflammatory activities. The levels of NO, TNF-α, and IL-6 in RAW264.7 cells were significantly increased after LPS stimulation ($P < 0.0001$), suggesting that the cell inflammation model could be successfully constructed by inducing RAW264.7 cells with 2 μg/mL LPS. As displayed in Figure 6b–d, after drug treatment, the levels of inflammatory cytokines were decreased, and RES, PPD-Lip, PPD-Lip@MNX, and PPD-Lip@RES could significantly inhibit the production of NO ($P < 0.0001$). The inhibitory activity of PPD-Lip@RES on NO production was stronger than that of PPD-Lip@MNX. In addition, RES and PPD-Lip @RES significantly decreased the levels of TNF-α ($P < 0.05$) and IL-6 ($P < 0.0001$), indicating that RES and PPD-Lip @RES had good anti-inflammatory activities and could effectively reduce the levels of inflammatory factors induced by LPS in RAW264.7 cells. The above results indicated that RES and PPD-Lip@RES could reduce the LPS-induced deformation of RAW264.7 cells by reducing the levels of inflammatory factors in cells, and had good anti-inflammatory activity, which was conducive to protecting hair follicles from the damage of inflammatory factors and restoring the homeostasis of hair follicle microenvironment.

In vivo Evaluation of Hair Growth Promotion

To explore the effect of RES and PPD-Lip@RES on the treatment of alopecia in vivo, the C57BL/6 mice telogen effluvium (TE) model was established, and the whole treatment schedule was displayed in Figure 7a. Due to the epidermis of C57BL/6 mice lacks melanocytes, the color change of its dorsal skin comes from the melanin synthesized by hair follicles. The activity of melanocytes in hair follicles was closely related to the hair follicle cycle, when the hair follicles were in telogen phase, their dorsal skin color appears pink. With the entry of hair follicle anagen phase, melanin begins to synthesize, and the dorsal skin color deepened, so the hair follicle growth progress of mice could be judged by the color of dorsal skin. As shown in Figure 7b, the dorsal skin color of each group on the 6^{th} day was pink after hair removal, indicating that the hair follicles were in the telogen phase. As time passed, the hair follicles gradually entered the anagen phase, and the dorsal skin color deepened, accompanied by hair regeneration. By the 12^{th} day, the dorsal skin of the MNX group became completely black, and hair regenerated on 15^{th} day. Although the hair growth rate of PPD-Lip @RES group was slower than that of MNX group, by the 30^{th} day, the hair of PPD-Lip@RES group almost covered the whole back area, while there were still uncovered areas on the back of MNX group. Overall, PPD-Lip@RES group gained the thickest hair at the endpoint of the experiment.

The strength and toughness of the regrowth hair of each group on the 30^{th} day were investigated through the "hair pull" test. As shown in Figure 7c, although the MNX group regenerated hair earlier, the new hair easily fell off. In contrast, the regrowth hair in PPD-Lip@RES groups was sturdy and tough, and was not easy to fall off.

As shown in Figure 7d, there was no significant change in the body weight of each group, and there was no erythema, edema, or necrosis on dorsal skin (Figure 7b), indicating the good skin safety of different formulations. Considering that the color of the dorsal skin of mice was positively correlated with the hair cycle, starting from the 9^{th} day, the skin color of each group of mice was scored, as shown in Figure 7e, the skin color score of the treatment groups was higher than that of the model group, indicating that drug treatment could accelerate the hair follicles enter the anagen phase.

The regrowth hair in each group was collected and weighed, as shown in Figure 7f. The hair weight of PPD-Lip @RES group was significantly higher than those of the other groups ($P < 0.05$). In addition, as displayed in Figure 7g, the hair shaft diameter of the drug administration group was significantly larger than that of the model group ($P < 0.0001$), and the hair shaft diameter of RES, PPD-Lip@MNX and PPD-Lip@RES groups was significantly larger than that of MNX group ($P < 0.001$). The hair shaft in PPD-Lip@RES group was significantly higher than that in PPD-Lip @MNX and RES groups ($P < 0.0001$). The morphology of regenerated hair in each group was observed by microscope and SEM, and the results showed that the hair of each group was healthy with complete hair scales (Figure 7h).

To further investigate the changes of the hair follicle cycle after hair regeneration in each group, the dorsal skin color was observed after shaving the new hair. As shown in Figure S5. The dorsal skin color of the model and MNX group was pink, indicating that all hair follicles had entered the telogen period. Significantly, the dorsal skin color in RES, PPD-Lip @MNX, and PPD-Lip@RES groups still had black areas, indicating that they could prolong the anagen period of hair follicles and contribute to the sustained growth of hair.

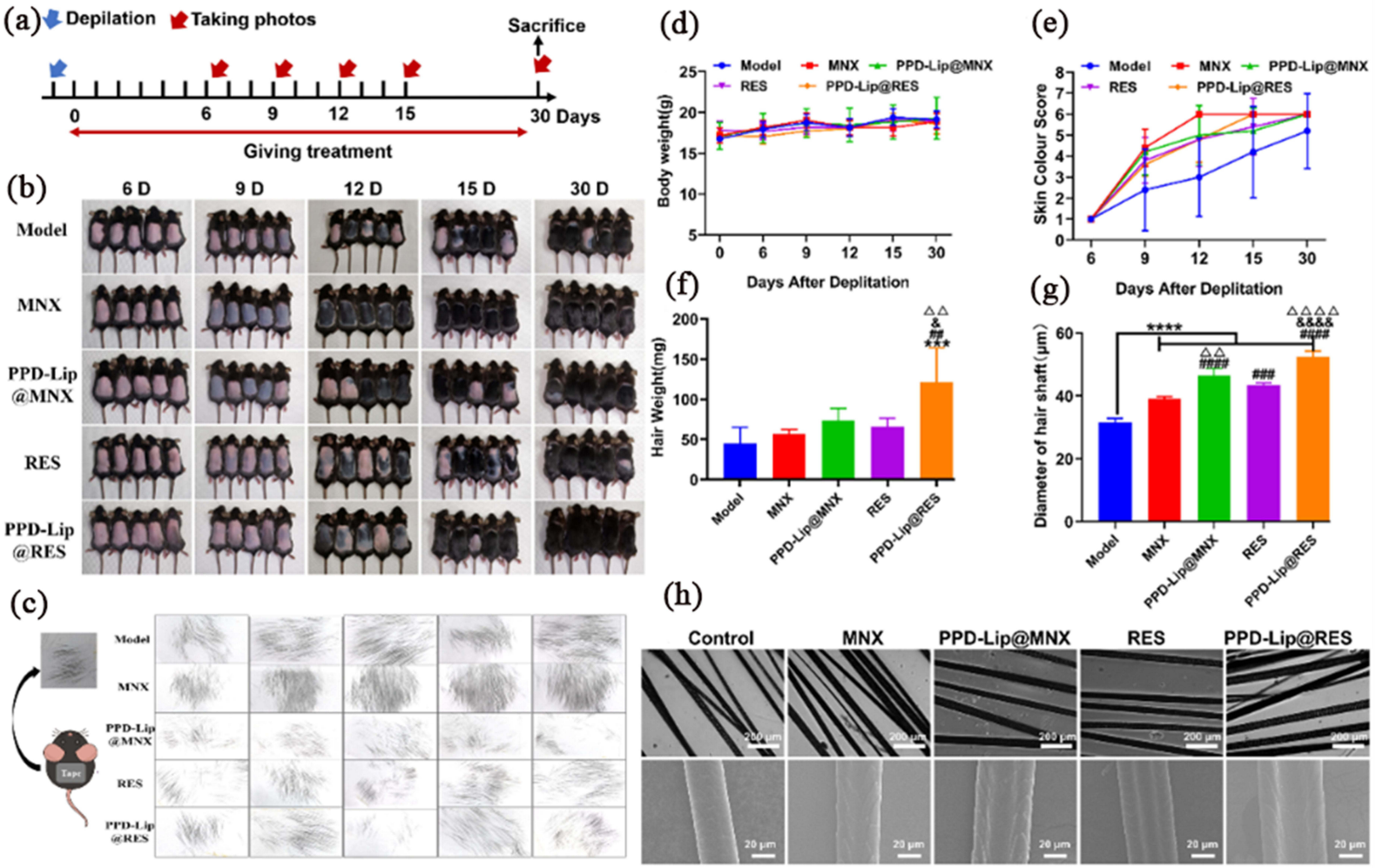

Figure 7 (**a**) Schematic diagram of the establishment of TE model and experimental schedule. (**b**) Photographs of TE mice treated with different formulations. (**c**) Hair loss of mice in each group after hair pull test by the tape assay. In vivo evaluation of promoting hair growth in TE mice by different formulations. (**d**) Body weight of mice; (**e**) Skin color score of mice. (**f**) The weight of regenerated hair. (**g**) Diameter of hair shaft. $^{***}P < 0.001$; $^{****}P < 0.0001$ vs Model. $^{\#\#}P < 0.01$; $^{\#\#\#}P < 0.001$; $^{\#\#\#\#}P < 0.0001$ vs MNX. $^{\&}P < 0.05$; $^{\&\&\&\&}P < 0.0001$ vs PPD-Lip@MNX. $^{\Delta\Delta}P < 0.01$; $^{\Delta\Delta\Delta\Delta}P < 0.0001$ vs RES. (**h**) Photo of hair shaft under inverted microscope (above); SEM images of regenerated hair shaft (below).

The skin thickness was closely related to the hair cycle. When the hair follicles were in the anagen phase, the skin thickness was thicker, and gradually thinner as the telogen phase enters.[25] The skin H&E staining results of each group were shown in Figure 8a, the skin of RES, PPD-Lip@MNX, and PPD-Lip@RES groups were thicker, with a larger number of hair follicles, and the hair follicles were deeply rooted in the deep layers of the skin. Quantitative analysis of the mouse skin thickness and hair bulb diameter (Figure 8b and c) revealed that the skin thickness and hair ball diameter of PPD-Lip@RES group were significantly greater than PPD-Lip@MNX, MNX, RES, and modal groups ($P < 0.05$). The evaluation results of hair follicle cycle stages showed that the percentage of hair follicles in the anagen phase in PPD-Lip @RES, RES, and PPD-Lip@MNX groups were higher than that of MNX and model groups (Figure 8d). The results suggested that although the MNX group could accelerate hair follicles to enter the anagen phase, it could not maintain the anagen phase. After hair regeneration, the hair follicles would enter the telogen phase again, resulting in thinner skin thickness and smaller hair bulb diameter. Nevertheless, PPD-Lip@RES could not only promote the transition of hair follicles from the telogen phase to the anagen phase but also maintain the anagen phase of hair follicles to promote continuous hair growth. The effect of PPD-Lip@RES on promoting hair regeneration was stronger than PPD-Lip@MNX.

Collagen, a vital constituent of the extracellular matrix (ECM) within hair follicles, played a pivotal role in preserving distinct cell phenotypes and facilitating the functioning of DP through intricate cellular interactions.[31] In addition, collagen could strengthen hair follicles and prevent hair loss. Masson's trichrome staining result showed that the collagen

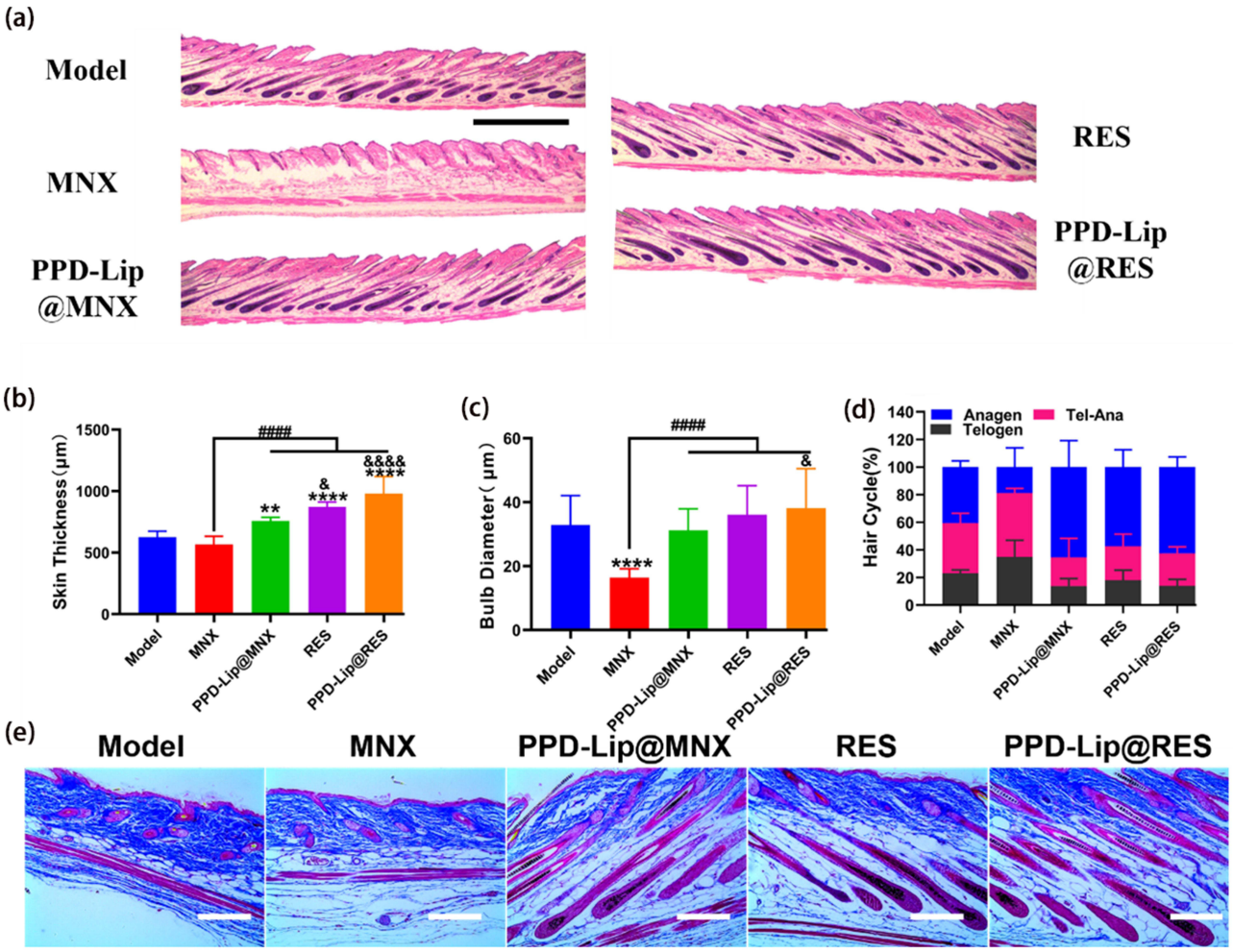

Figure 8 Histological analysis in TE mice. (**a**) H&E staining images, scale bar = 1000 μm. (**b**) Skin thickness. (**c**) Bulbs diameter. (**d**) Percentage of hair cycle stage in each group. (**e**) Masson's trichrome staining images, scale bar = 200 μm. $^{**}P < 0.01$; $^{****}P < 0.0001$ vs Model. $^{\#\#\#\#}P < 0.0001$ vs MNX. $^{\&}P < 0.05$; $^{\&\&\&\&}P < 0.0001$ vs PPD-Lip @MNX.

tightly surrounded the hair follicles in the PPD-Lip@RES group (Figure 8e), which could provide approving ECM for hair follicle growth, promote hair growth, and help to stabilize the hair follicle to prevent hair loss.

Hair follicle cell proliferation was an important feature of the anagen phase. Ki67 was one of the essential markers of hair follicle cell proliferation, which could be evaluated by immunofluorescence staining to assess whether or not hair follicles were in the anagen phase.[25] In addition, the Wnt/β-catenin signaling pathway was one of the most critical pathways controlling hair growth and cycle, regulating the proliferation and migration of hair matrix, DP, and HFSCs through autocrine or paracrine, which could induce hair follicles to transform from the telogen phase to the anagen phase and maintain growth period. The expression of β-catenin could be used to evaluate whether the Wnt/β-catenin signaling pathway was activated. Keratin was the main component of hair formation, which was directly related to the development and differentiation of hair follicle epithelium. Furthermore, keratin regulates communication between cells. K5 belongs to type II keratin, which was expressed in the early anagen stage of hair follicle epidermal cells. As shown in Figure 9a–c, PPD-Lip@RES, RES, and PPD-Lip@MNX could up-regulate the expression of Ki67, β-catenin, and K5, indicating that they promoted hair regeneration by promoting cell proliferation and activating Wnt/β-catenin signaling pathway, accelerating the entry of hair follicle anagen phase. In addition, they also could maintain hair follicle growth by promoting epidermal cell growth.

The formation of blood vessels around the hair follicle was closely related to the hair follicle cycle. When the hair follicle was in the growth phase, the density and volume of the blood vessels around the hair follicle were the largest. With the entry of the catagen and telogen phase, the number of blood vessels significantly reduced and even disappeared. Enhancing vascularization around hair follicles could provide sufficient nutrients and growth factors to meet the nutritional need of

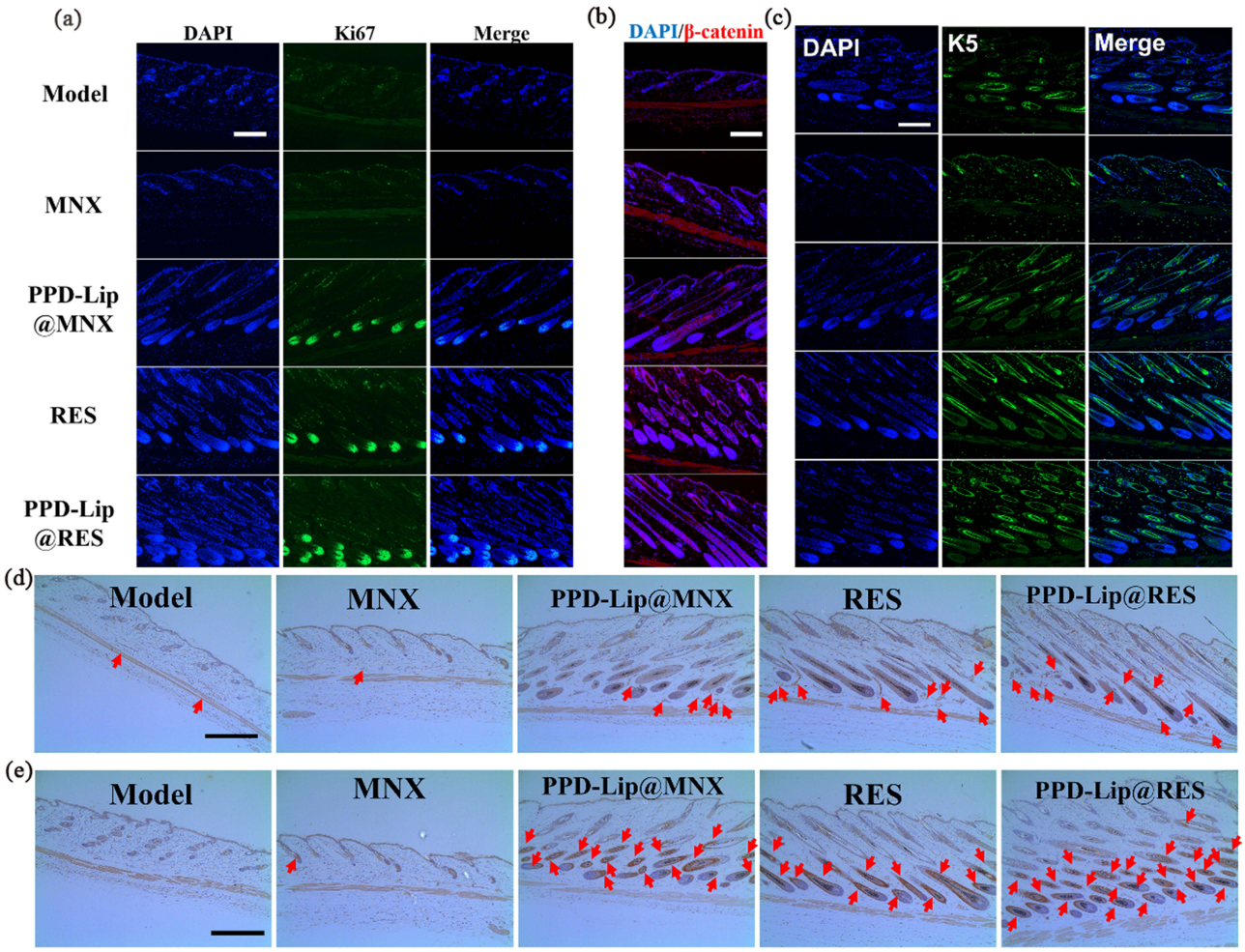

Figure 9 Expression of Ki67 (**a**), β-catenin (**b**) or K5 (**c**) in dorsal skin of mice, scale bar = 200 μm. Immunohistochemical results of CD31 (**d**), or CK19 (**e**) expression in the dorsal skin of TE mice. The red arrow indicated the expression of CD31 or CK19, scale bar = 400 μm.

hair follicle growth, which was particularly important for accelerating hair growth and increasing hair follicle density. CD31 was a marker of vascular endothelial cells, which could be used to determine the degree of vascularization.

HFSCs were essential for the maintenance and regulation of hair follicle cycle, and the formation of new hair shafts depends on the activation of HFSCs. When the hair follicles were in the catagen and telogen phase. In contrast, HFSCs will enter the activated state after entering the anagen phase. The high expression of CK19, a marker of HFSCs, implied the good status of HFSCs.

As shown in Figure 9d and e, the expression of CD31 and CK19 was up-regulated in PPD-Lip@RES, RES, and PPD-Lip @MNX groups, and the effect of PPD-Lip@RES was superior to that of PPD-Lip@MNX. These results indicated that PPD-Lip @RES could promote angiogenesis, increasing the microcirculation blood supply of hair follicles. In addition, they could activate HFSCs to promote the transition of hair follicles from the telogen phase to the anagen phase, thus promoting hair growth.

As displayed in Figure 10a, we used 5 mg/mL of testosterone propionate (TTP) as the modeling agent to construct a severe AGA mouse model. The result showed that compared with the control group, the darkening time of the dorsal skin color in the model group was extended from 25 days to 50 days (Figure 10b), and the regenerated hair was unable to cover their dorsal skin on the 70th day, indicating the successful construction of a severe AGA mouse model. In the drug treatment groups, hair regeneration began on the 40th day, and the hair coverage area gradually increased in a time-dependent matter. The coverage area of regenerated hair in the RES and FIN group was similar and significantly greater than that of the model group. In addition, the exposed skin color of the RES group was darker, while the exposed skin color of the FIN group was pink, indicating that RES could accelerate the hair follicles enter the anagen phase. Notably, compared with the RES and FIN groups, PPD-Lip@RES group had a larger hair coverage and darker dorsal skin color. On day 60, the regenerated hair in PPD-Lip@RES group almost covered the entire back area of the mice, while there were still uncovered area in the RES and FIN groups. These results indicated that PPD-Lip@RES could accelerate hair follicles into the anagen phase and had the best hair regeneration effect.

As shown in Figure 10c, there was no significant change in mouse body weight throughout the entire experimental cycle, indicating that each administration group had good skin safety. The dorsal skin color score result showed that since the 30th day, the skin color score of the drug administration groups came much higher than that of the model group, indicating that drug treatment could accelerate the hair follicle to enter the anagen phase (Figure 10d). The quantitative results were consistent with the results we had observed from Figure 10b.

The quantitative results of the coverage area of new hair from day 60 to 70 were shown in Figure 10e. On day 60, the hair coverage area of five mice in PPD-Lip@RES group was more than 80%, while only four mice in FIN and RES groups had more than 50%, and only two mice in the model group had new hair, with one mouse had a hair coverage area less than 50%. On day 70, the hair coverage area of PPD-Lip@RES group was close to 100%, which was significantly higher than that of the control group (about 82%). And the average hair coverage of the RES was about 83%, which was higher than that of the FIN group (about 71%) and model group (about 32%). In general, the hair coverage area of FIN group and RES group was higher than that of model group in a time-dependent manner, but the regeneration hair coverage area was still significantly lower than that of PPD-Lip@RES group. These results indicated that androgen could delay hair regeneration in mice, and PPD-Lip @RES could significantly promote hair regeneration in AGA model mice, which was much better than the FIN group.

Hair growth of mice at different stages was observed by hair detector, as shown in Figure 10f. Hair follicles in the model group were still closed at day 40, with almost no new hair. In the PPD-Lip@RES group, although there was no significant hair regeneration observed with naked eye on day 30, new hair could be observed under the hair detector, and the hair density was significantly higher than that of FIN, RES, model, and control groups. In addition, with the extension of time, hair continued to grow and could be observed with naked eye. On day 45, new hair was observed under the hair microscope in the FIN group, but the hair density was significantly lower than that in PPD-Lip@RES group. On day 70, compared with the other groups, the hair in group PPD-Lip@RES was dense, and the hair stem was thicker. These results showed that PPD-Lip@RES could promote the regeneration of healthy hair in severe AGA model mice.

Since the hair of the model mice was too short to pull, hair pull tests were only conducted in the other groups. As shown in Figure 10g, the pull-down hair in RES and PPD-Lip@RES groups was similar to that of the control group, implying new hair was strong, sturdy, and not easily pulled off. Comparatively, the pull-down hair in FIN group was less than that of RES group, because the regrowth hair in FIN group was shorter than that in RES group. All in all, the PPD-

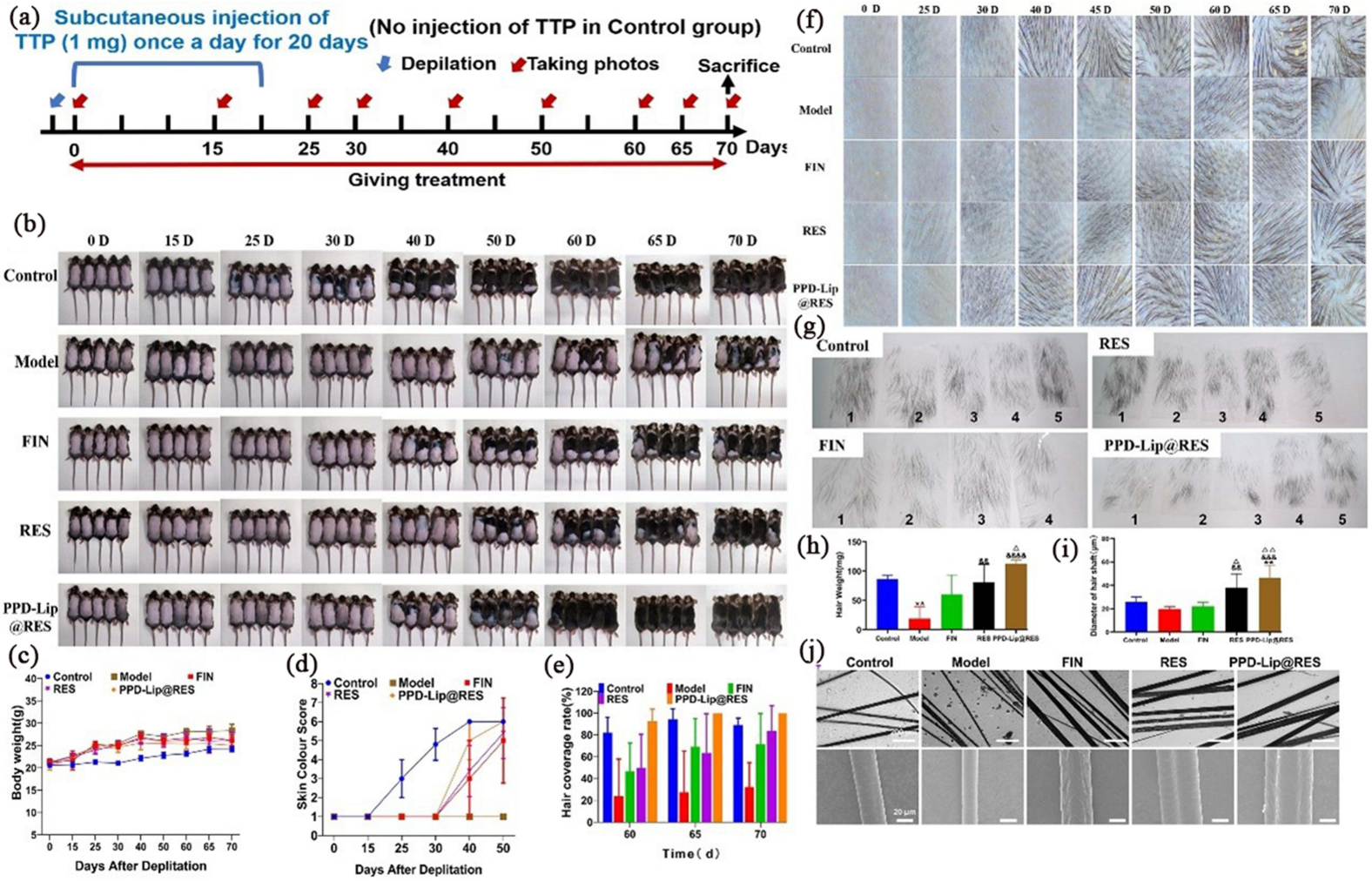

Figure 10 In vivo evaluation of promoting hair growth in AGA mice by different formulations. (**a**) Schematic diagram of the establishment of severe AGA model and mice treatment schedule. (**b**) Photographs of AGA mice. (**c**) Body weight of mice. (**d**) Skin color score of mice. (**e**) Hair coverage rate. (**f**) Detection of hair regeneration in mice by scalp detector. (**g**) Hair pull test by the tape assay in mice treated with various formulations. Evaluation of regenerated hair in each group. (**h**) The weight of regenerated hair. (**i**) Diameter of the hair shaft. (**j**) Photo of hair shaft under an inverted microscope, scale bar = 200 μm (above). SEM images of the regenerated hair shaft, scale bar = 20 μm (below). $^{**}P < 0.01$ vs Control. $^{\&\&}P < 0.01$; $^{\&\&\&}P < 0.001$; $^{\&\&\&\&}P < 0.0001$ vs Model. $^{\Delta}P < 0.05$; $^{\Delta\Delta}P < 0.01$ vs FIN.

https://doi.org/10.2147/IJN.S477820

Lip@RES group not only exhibited a faster hair growth rate but also stronger and tougher hair, indicating that PPD-Lip @RES could promote the hair regeneration and preventing hair shedding.

As shown in Figure 10h–j, the regrowth hair of mice in each group with the same area was collected and weighed, and the hair shaft diameter was measured too. The new hair morphology was observed by microscope and SEM. The hair weight of the model group was significantly lower than that of the other groups ($P < 0.01$), which indicated that androgens could cause hair follicle miniaturization and hair thinning. The hair weight and diameter in PPD-Lip@RES and RES groups were significantly larger than those in the model group and FIN group ($P < 0.05$). Among them, the hair shaft of the PPD-Lip@RES group was even significantly thicker than that of the control group ($P < 0.01$) with the hair scales intact, indicating that the PPD-Lip@RES group had a superior effect on promoting hair growth.

As shown in Figure S6, the dorsal skin color after shaving in the model group and control group was pink, indicating that the hair follicles were in a telogen phase. In contrast, FIN, RES, and PPD-Lip@RES groups still had black areas, indicating that the hair follicles were still in the anagen stage, suggesting that it could not only promote the transition of hair follicles from the telogen phase to the anagen phase in AGA mice but also maintain the growth stage.

As shown in Figure 11a–d, the skin thickness of the model group was significantly thinner than that of the other groups, the number of hair follicles was less, hair bulb diameter was significantly lower and most hair follicles were in the telogen stage, indicating that the AGA model was successfully constructed. It was noteworthy that after drug treatment, the skin thickened, the diameter of the hair bulb increased, the number of hair follicles in the anagen phase increased, and the hair follicles rooted in the

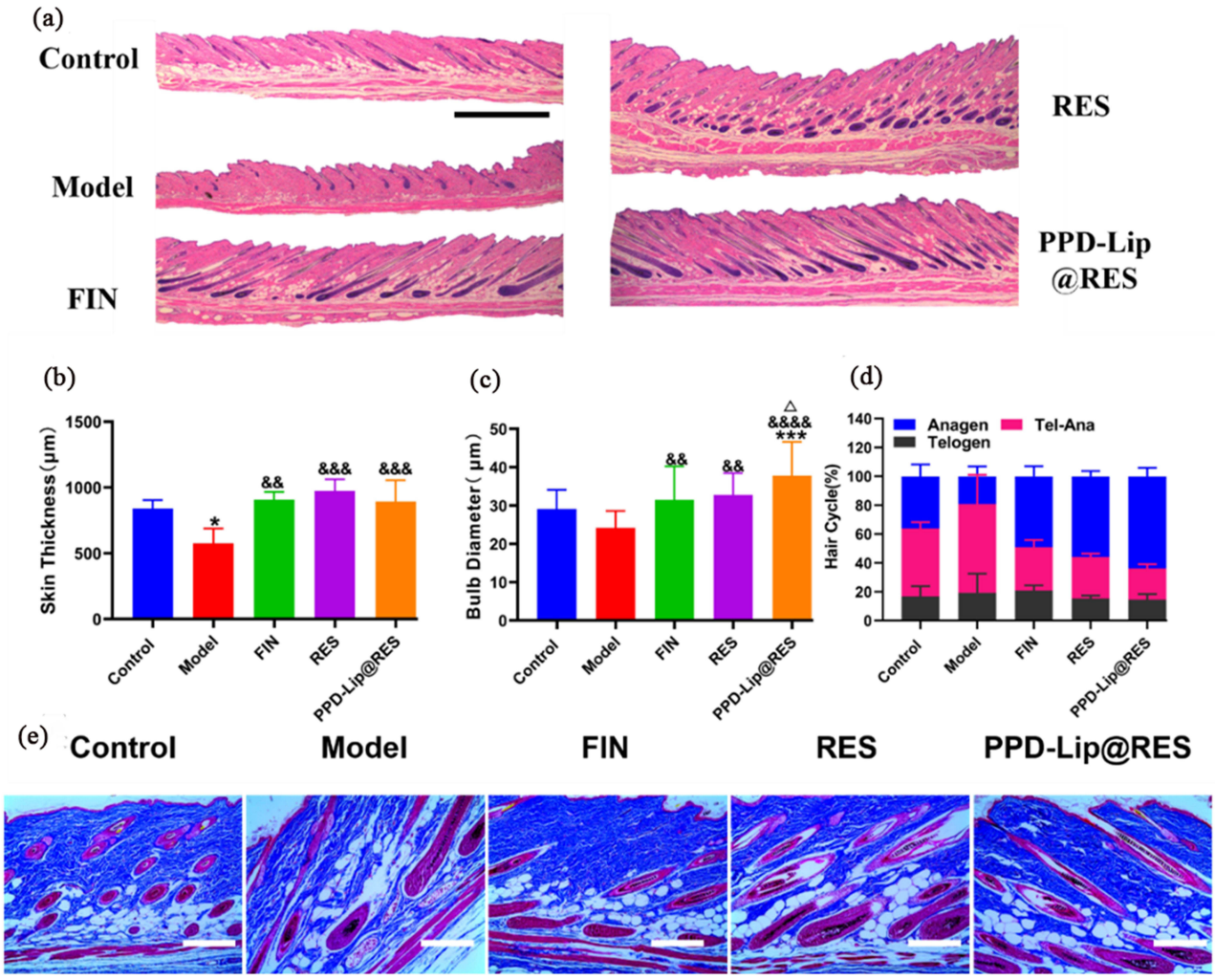

Figure 11 Histological analysis in AGA mice. (**a**) H&E staining images, scale bar = 1000 μm. (**b**) Skin thickness. (**c**) Bulbs diameter. (**d**) The percentage of HF at each hair cycle stage. (**e**) Masson's trichrome staining images, scale bar = 200 μm. *$P < 0.05$ vs Control. $^{\&\&}P < 0.01$; $^{\&\&\&}P < 0.001$; $^{\&\&\&\&}P < 0.0001$ vs Model. $^{\triangle}P < 0.05$ vs FIN.

deep layer of skin, implying that drug treatment could effectively treat AGA. Among them, the hair bulb diameter and percentage of anagen phase hair follicles in the PPD-Lip@RES group were significantly higher than those in the FIN group, indicating the optimal therapeutic effect. Masson staining showed that the collagen fibers in the PPD-Lip@RES group were neatly arranged around the hair follicles (Figure 11e), which could effectively strengthen the hair follicles and prevent hair loss.

The pathogenesis of AGA involved multiple pathways and factors, including oxidative stress, inflammation, angiogenesis, etc.[32] As an important pathogenic factor, oxidative stress was related to cell dysfunction, cellular senescence, and migration.[4] According to the literature,[33] dihydrotestosterone (DHT) in the hair follicles of AGA patients could stimulate the secretion of hair growth inhibitory factors. At the same time, oxidative stress and ROS accumulation may inhibit growth factor signaling in cells, thereby affecting hair growth. Therefore, evaluating the effects of drugs on oxidative stress in AGA mice was of great significance.

Dihydroethidium (DHE), as a superoxide anion probe, could freely penetrate the cell membrane and be oxidized by ROS to ethylene oxide, which could be incorporated into the nuclear DNA to form red fluorescence. Therefore, DHE staining could be used to determine the oxidative state of mouse skin. As shown in Figure S7, the red fluorescence of the model group was significantly higher than that of the other groups, indicating that the ROS level in the model group was the highest. After drug treatment, the ROS level decreased, resulting in a decrease in fluorescence. Among them, there was almost no red fluorescence was detected in RES group and PPD-Lip@RES group, indicating RES and PPD-Lip@RES had good antioxidant activity and could effectively eliminate ROS in the skin of AGA mice, helped to prevent premature aging of DPCs and promoted hair growth.

As shown in Figure 12a–c, RES and PPD-Lip@RES could significantly upregulate the expression of Ki67, β-catenin, and K5, suggesting that they could promote cell proliferation, activate Wnt/β-catenin signaling pathway, increase the

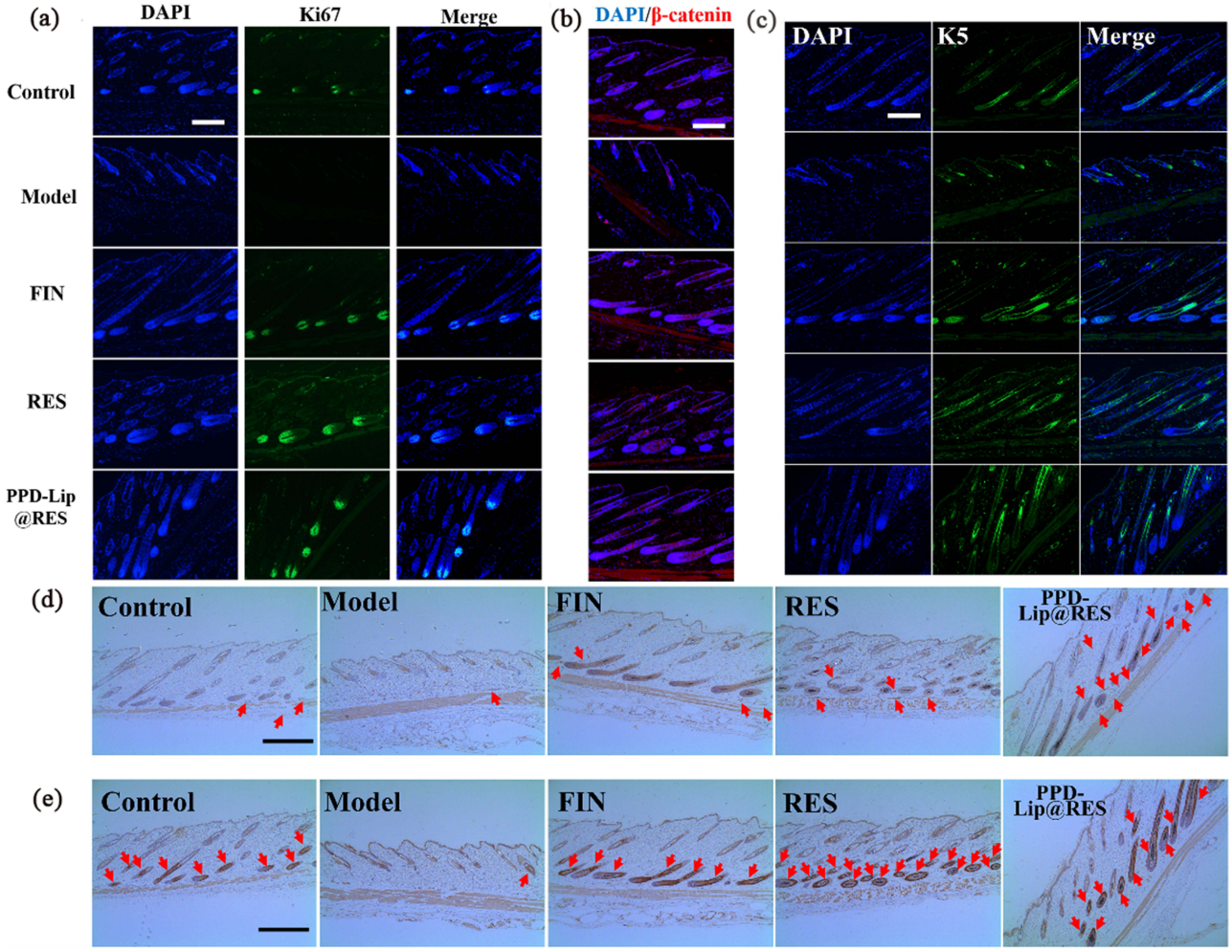

Figure 12 Expression of Ki67 (**a**), β-catenin (**b**) or K5 (**c**) in the dorsal skin of AGA mice, scale bar = 200 μm. Immunohistochemical results of CD31 (**d**), or CK19 (**e**) expression in the dorsal skin of AGA mice. The red arrow indicated the expression of CD31 or CK19, scale bar = 400 μm.

growth of epidermal cells, and promote the transition of hair follicles from telogen to anagen phase, thereby promoting hair regeneration.

The immunohistochemical results showed that the expression levels of CD31 and CK19 in the model group were extremely low (Figure 12d and e), indicating that androgen could cause insufficient vascularization around the hair follicles and inhibit the transition of hair follicles from the telogen phase to the anagen phase. On the contrary, the expression of CD31 and CK19 in PPD-Lip@RES group was significantly higher than that in the model and control groups, indicating vascularization increased and HFSCs activated. The results showed that PPD-Lip@RES could restore hair follicle microcirculation by inducing angiogenesis, providing nutrients for hair growth, and promoting hair follicle growth. In addition, PPD-Lip@RES could activate HFSCs, maintain the hair follicle in the anagen phase, and promote sustained hair growth.

Wnt3a, β-catenin, and VEGF were hair growth-promoting genes. FGF5 could directly act on matrix cells, inhibit their proliferation, or induce apoptosis, and then induce hair follicle degeneration.[34] BMP2, as a negative regulator of hair growth, could delay the entry of the anagen phase of hair follicles by inhibiting the proliferation of hair follicle cells and maintaining the resting state of HFSCs to inhibit hair growth.[35]

As shown in Figure S8, the expression of hair growth-promoting genes, including Wnt3a, β-catenin, and VEGF in the skin was up-regulated in the drug administration groups. In contrast, the expression of hair growth inhibiting genes, FGF5 and BMP2, was down-regulated. Among them, PPD-Lip@RES could significantly up-regulate the expression of Wnt3a and VEGF ($P < 0.05$), suggesting that PPD-Lip@RES could promote the hair follicle to enter the anagen phase and delay the hair follicle to enter the telogen phase, thus promoting hair regeneration.

DKK-1 was an inhibitor of the Wnt pathway. Overexpression of DKK-1 could inhibit the Wnt signaling pathway, leading to apoptosis of outer root sheath cells in hair follicles, and promoting early regression of hair follicles.[36] Kwack et al found that DHT in the hair loss area could induce DPCs to secrete DKK-1,[37] inhibit the growth of hair root sheath cells, and induce apoptosis of keratinocytes. In addition, TGF- β1 was a critical factor in the onset of AGA.[38] TGF- β1 could cause fibrosis in the surrounding tissues of hair follicles, induce cell apoptosis, cause hair follicles to shrink and become smaller, promote hair follicles to enter the catagen and telogen stages early, shorten the anagen phase, and then lead to hair loss. Therefore, we examined the expression of the hair growth-inhibiting genes DKK-1 and TGF- β1 in the skin of AGA mice.

As shown in Figure S9, PPD-Lip@RES significantly up-regulated the hair growth-promoting expression of Wnt3a, β-catenin, and VEGF in the skin of AGA mice. The expression of DKK-1 and TGF-β1 in the model group was higher than that of the control group, indicating that androgens could upregulate DKK-1 and TGF-β1. While drug treatment groups could down-regulate the expression of DKK-1 and TGF-β1, indicating that drug therapy could promote hair follicles to enter the anagen phase and accelerate hair growth by inhibiting the expression of hair growth inhibitory genes. The possible reason that the expression levels of DKK-1 and TGF-β1 in the drug treatment groups lower than the control group was that the control group was not affected by androgens so that the hair follicle cycle was normally advanced. By the 25th day, the hair follicles had regenerated and entered the anagen phase. As time went on, the hair follicles gradually entered the catagen and telogen phases. Therefore, the expression of negative regulatory genes was higher than that of the drug treatment group, which was in the anagen phase. These results indicated that PPD-Lip@RES could promote hair follicles to enter the anagen phase and delay the entry of the telogen phase by up-regulating the expression of hair growth-related genes and down-regulating the expression of negative regulatory genes, thus promoting sustainable hair growth.

Conclusion

Based on the complicated pathogenesis of hair loss, utilizing comprehensive strategies involving multi-mechanisms of anti-hair loss might better achieve the treatment of hair loss. In this study, we constructed a multi-mechanism nanovesicle PPD-Lip@RES, which has prominent antioxidant, anti-inflammatory, pro-proliferations, and pro-angiogenesis activities to promote hair growth through various mechanisms. Our results confirmed that PPD-Lip@RES could effectively deliver RES to the skin and remain long in the skin, thus serving as a drug reservoir for sustained effectiveness. It facilitated hair growth in vitro and in vivo by enhancing cell proliferation, initiating the Wnt/β-catenin signaling pathway, promoting angiogenesis, and activating HFSCs. Moreover, PPD-Lip@RES could improve the oxidative stress and inflammatory status, and thus restore the microenvironmental homeostasis of the hair follicles. The results of in vivo efficacy in the

telogen effluvium model showed that the PPD-Lip@RES group gained tougher new hair than the MNX group. More importantly, it also has a good therapeutic effect on the severe AGA model, with faster hair growth rate, denser hair cover, and stronger new hair than those of the topical FIN group as well as the healthy control group. Overall, PPD-Lip @RES with a comprehensive strategy, targeting the multi-mechanisms of alopecia, could play a superior role in treating normal and even severe hair loss, meanwhile providing a new direction for the clinical treatment of hair loss.

However, certain limitations warrant further investigation. Firstly, more extensive exploration based on animal experiments is needed to validate the generalizability of our findings. Additionally, the exact underlying mechanisms such as the detailed interactions with cell signaling pathways remain incompletely understood. Future research would focus on elucidating these pathways with greater precision to optimize the therapeutic potential of PPD-Lip@RES in clinical applications.

Acknowledgment

This work was supported by Guangzhou Science and Technology Key Program (No. 2023B03J0022), the National Natural Science Foundation of China (No. 82273870, 82104080, and 81973264), Guangdong Basic and Applied Basic Research Foundation (No. 2023A1515012909), Guangdong Provincial Key Laboratory of Construction Foundation (No. 2023B1212060022), Yunnan Fundamental Research Projects (No. 202401AT070156).

Disclosure

The authors report no conflicts of interest in this work.

References

1. Zito PM, Raggio BS. Hair transplantation. StatPearls. Treasure Island (FL) ineligible companies. Disclosure: Blake Raggio declares no relevant financial relationships with ineligible companies.: StatPearls Publishing Copyright © 2023, StatPearls Publishing LLC.; 2023.
2. Chai M, Jiang M, Vergnes L, et al. Stimulation of hair growth by small molecules that activate autophagy. *Cell Rep*. 2019;27(12):3413–21.e3. doi:10.1016/j.celrep.2019.05.070
3. Wagener FA, Carels CE, Lundvig DM. Targeting the redox balance in inflammatory skin conditions. *Int J Mol Sci*. 2013;14(5):9126–9167. doi:10.3390/ijms14059126
4. Upton JH, Hannen RF, Bahta AW, Farjo N, Farjo B, Philpott MP. Oxidative stress-associated senescence in dermal papilla cells of men with androgenetic alopecia. *J Investigative Dermatol*. 2015;135(5):1244–1252. doi:10.1038/jid.2015.28
5. Yang YC, Fu HC, Wu CY, Wei KT, Huang KE, Kang HY. Androgen receptor accelerates premature senescence of human dermal papilla cells in association with DNA damage. *PLoS One*. 2013;8(11):e79434. doi:10.1371/journal.pone.0079434
6. Lee TK, Kim B, Kim DW, et al. Effects of decursin and angelica gigas nakai root extract on hair growth in mouse dorsal skin via regulating inflammatory cytokines. *Molecules*. 2020;25(16):3697.
7. Bejaoui M, Taarji N, Saito M, Nakajima M, Isoda H. Argan (Argania Spinosa) press cake extract enhances cell proliferation and prevents oxidative stress and inflammation of human dermal papilla cells. *J Dermatological Sci*. 2021;103(1):33–40. doi:10.1016/j.jdermsci.2021.06.003
8. Lephart ED. Resveratrol, 4' acetoxy resveratrol, R-equol, racemic equol or S-equol as cosmeceuticals to improve dermal health. *Int J Mol Sci*. 2017;18(6):1193. doi:10.3390/ijms18061193
9. Heenatigala Palliyage G, Singh S, Ashby CR, Tiwari AK, Chauhan H. Pharmaceutical topical delivery of poorly soluble polyphenols: potential role in prevention and treatment of melanoma. *AAPS Pharm Sci Tech*. 2019;20(6):250. doi:10.1208/s12249-019-1457-1
10. Huang WY, Huang YC, Huang KS, et al. Stress-induced premature senescence of dermal papilla cells compromises hair follicle epithelial-mesenchymal interaction. *J Dermatological Sci*. 2017;86(2):114–122. doi:10.1016/j.jdermsci.2017.01.003
11. Tian Q, Quan P, Fang L, Xu H, Liu C. A molecular mechanism investigation of the transdermal/topical absorption classification system on the basis of drug skin permeation and skin retention. *Int J Pharm*. 2021;608:121082. doi:10.1016/j.ijpharm.2021.121082
12. Hung CF, Lin YK, Huang ZR, Fang JY. Delivery of resveratrol, a red wine polyphenol, from solutions and hydrogels via the skin. *Biol Pharm Bull*. 2008;31(5):955–962. doi:10.1248/bpb.31.955
13. Santos AC, Rodrigues D, Sequeira JAD, et al. Nanotechnological breakthroughs in the development of topical phytocompounds-based formulations. *Int J Pharm*. 2019;572:118787. doi:10.1016/j.ijpharm.2019.118787
14. Zhang X, Li S, Dong Y, Rong H, Zhao J, Hu HA. A multifunctional cholesterol-free liposomal platform based on protopanaxadiol for alopecia therapy. *Nano Res*. 2022;15(10):9498–9510.
15. Tang P, Wang X, Zhang M, et al. Activin B stimulates mouse vibrissae growth and regulates cell proliferation and cell cycle progression of hair matrix cells through ERK Signaling. *Int J Mol Sci*. 2019;20(4):853. doi:10.3390/ijms20040853
16. Zhang X, Zhao J. Biological activities and detoxification mechanisms of Clerodendrum chinense var. simplex, marsdenia tenacissima and arundina graminifolia: the Dai antidotes. *Acta Scientiarum Naturalium Universitatis Sunyatseni*. 2023;62(3):89–99.
17. Müller-Röver S, Handjiski B, van der Veen C, et al. A comprehensive guide for the accurate classification of murine hair follicles in distinct hair cycle stages. *J Investigative Dermatol*. 2001;117(1):3–15. doi:10.1046/j.0022-202x.2001.01377.x
18. Kalave S, Chatterjee B, Shah P, Misra A. Transdermal delivery of macromolecules using nano lipid carriers. *Curr Pharm Des*. 2021;27(42):4330–4340. doi:10.2174/1381612827666210820095330

19. Madaan A, Verma R, Singh AT, Jaggi M. Review of hair follicle dermal papilla cells as in vitro screening model for hair growth. *Int J Cosmet Sci*. 2018;40(5):429–450. doi:10.1111/ics.12489
20. Chen Y, Huang J, Chen R, et al. Sustained release of dermal papilla-derived extracellular vesicles from injectable microgel promotes hair growth. *Theranostics*. 2020;10(3):1454–1478. doi:10.7150/thno.39566
21. Yano K, Brown LF, Detmar M. Control of hair growth and follicle size by VEGF-mediated angiogenesis. *J Clin Invest*. 2001;107(4):409–417. doi:10.1172/JCI11317
22. Ji S, Zhu Z, Sun X, Fu X. Functional hair follicle regeneration: an updated review. *Signal Trans Target Ther*. 2021;6(1):66. doi:10.1038/s41392-020-00441-y
23. Yuan A, Xia F, Bian Q, et al. Ceria nanozyme-integrated microneedles reshape the perifollicular microenvironment for androgenetic alopecia treatment. *ACS nano*. 2021;15(8):13759–13769. doi:10.1021/acsnano.1c05272
24. Deng Z, Chen M, Liu F, et al. Androgen receptor-mediated paracrine signaling induces regression of blood vessels in the dermal papilla in androgenetic alopecia. *J Investigative Dermatol*. 2022;142(8):2088–99.e9. doi:10.1016/j.jid.2022.01.003
25. Fu D, Huang J, Li K, et al. Dihydrotestosterone-induced hair regrowth inhibition by activating androgen receptor in C57BL6 mice simulates androgenetic alopecia. *Biomed Pharmacothe*. 2021;137:111247. doi:10.1016/j.biopha.2021.111247
26. You J, Woo J, Roh KB, et al. Assessment of the anti-hair loss potential of Camellia japonica fruit shell extract in vitro. *Int J Cosmet Sci*. 2023;45(2):155–165. doi:10.1111/ics.12827
27. Williams R, Pawlus AD, Thornton MJ. Getting under the skin of hair aging: the impact of the hair follicle environment. *Experim Dermatol*. 2020;29(7):588–597. doi:10.1111/exd.14109
28. Chew EGY, Lim TC, Leong MF, et al. Observations that suggest a contribution of altered dermal papilla mitochondrial function to androgenetic alopecia. *Experim Dermatol*. 2022;31(6):906–917. doi:10.1111/exd.14536
29. Wood JM, Decker H, Hartmann H, et al. Senile hair graying: H2O2-mediated oxidative stress affects human hair color by blunting methionine sulfoxide repair. *FASEB J*. 2009;23(7):2065–2075. doi:10.1096/fj.08-125435
30. Doles J, Storer M, Cozzuto L, Roma G, Keyes WM. Age-associated inflammation inhibits epidermal stem cell function. *Genes Dev*. 2012;26(19):2144–2153. doi:10.1101/gad.192294.112
31. Abreu CM, Marques AP. Recreation of a hair follicle regenerative microenvironment: successes and pitfalls. *Bioeng Transl Med*. 2022;7(1):e10235. doi:10.1002/btm2.10235
32. Kash N, Leavitt M, Leavitt A, Hawkins SD, Roopani RB. Clinical patterns of hair loss in men: is dihydrotestosterone the only culprit? *Dermatol Clinics*. 2021;39(3):361–370. doi:10.1016/j.det.2021.03.001
33. Cwynar A, Olszewska-Słonina DM, Czajkowski R. The impact of oxidative stress in androgenic alopecia in women. *Postepy dermatologii i alergologii*. 2020;37(1):119–120. doi:10.5114/ada.2019.81685
34. Harshuk-Shabso S, Dressler H, Niehrs C, Aamar E, Enshell-Seijffers D. Fgf and Wnt signaling interaction in the mesenchymal niche regulates the murine hair cycle clock. *Nat Commun*. 2020;11(1):5114. doi:10.1038/s41467-020-18643-x
35. Plikus MV, Mayer JA, de la Cruz D, et al. Cyclic dermal BMP signalling regulates stem cell activation during hair regeneration. *Nature*. 2008;451(7176):340–344. doi:10.1038/nature06457
36. Premanand A, Reena Rajkumari B. Androgen modulation of Wnt/β-catenin signaling in androgenetic alopecia. *Archiv Dermatol Res*. 2018;310(5):391–399. doi:10.1007/s00403-018-1826-8
37. Kwack MH, Sung YK, Chung EJ, et al. Dihydrotestosterone-inducible dickkopf 1 from balding dermal papilla cells causes apoptosis in follicular keratinocytes. *J Investigative Dermatol*. 2008;128(2):262–269. doi:10.1038/sj.jid.5700999
38. Inui S, Fukuzato Y, Nakajima T, Yoshikawa K, Itami S. Androgen-inducible TGF-beta1 from balding dermal papilla cells inhibits epithelial cell growth: a clue to understand paradoxical effects of androgen on human hair growth. *FASEB J*. 2002;16(14):1967–1969. doi:10.1096/fj.02-0043fje